Developments in silo design for the safe and efficient storage and handling of grain

A. W. Roberts*

Abstract

This paper presents an overview of some recent developments in the technology of bulk solids handling as it relates to the grain industry. The paper focuses on silo and discharge equipment design, emphasising the need to understand the relevant properties of the grain and how these relate to silo geometry and discharge flow pattern to generate the load patterns exhibited in the silo walls. With the emphasis on grain conditioning procedures, such as aeration, to control grain quality, it is important to also take note of the influence of any such grain conditioning on the bulk storage and flow properties of the grain. Any change in the flow properties of the grain can influence, sometimes significantly, the pressures and loadings occurring in silo walls. The matter of structural integrity and safety of the silo and the efficiency and reliability of the discharge equipment, such as feeders used to control discharge rate, are of paramount importance.

The paper includes a brief review of discharge flow patterns in bins and silos and presents an overview of the complex pressure loading patterns in silo walls. Single outlet, multiple outlet symmetric silos are discussed as well as silos with eccentric loading due to either non-symmetric loading, or silos with eccentric discharge openings. Brief mention is made of the relevant flow properties such as angles of internal friction, bulk strength and friction angles between the grain and silo walls. Particular mention is made of the influence of grain moisture content variations, interstitial air, and temperature variations on the pressures and hence stresses occurring in silo walls.

Methods of controlling loads in tall, single and multi-outlet silos are discussed. Particular mention is made of the use of anti-dynamic tubes to control the flow pattern and, hence, control the magnitude of the wall pressures generated during discharge.

A recurring problem in bins and silos is the phenomenon of 'silo-quaking', a term used to describe pulsating loads which may be experienced during discharge. If the frequency of the flow pulsations is in harmony with any of the natural frequencies of the structure, severe dynamic loads and stresses can occur. The various mechanisms of 'silo quaking' will be outlined and methodologies to determine the magnitude and distributions of the dynamic loads will be given.

The paper will be illustrated by results from tests performed on pilot scale model silos, as well as by case studies drawn from field experience.

Introduction

Bulk materials handling operations are a key function in agricultural grain production. The capital costs of storage and handling plant are quite substantial, so too are the operating and running costs. With the emphasis on grain quality, it is not only important that attention be given to the maintenance of appropriate grain conditioning during storage, but also to the design of safe and functional storage and handling plant which ensures efficient and reliable operation. A full understanding of modern technology of silo and handling plant design, which takes account of the relevant physical properties of the granular materials under the varying environmental conditions during storage, is essential.

Over the past three decades much progress has been made in the theory and practice of bulk solids handling. Test procedures for determining the strength and flow properties of bulk solids have been developed and analytical methods have been established to aid the design of bulk solids storage and discharge equipment. Much progress has also been made in the understanding of the complex nature of loading conditions that may be generated in walls of storage bins and silos. There are now reliable theories and associated design procedures that may be applied, with confidence, to the solutions of practical silo design problems. Yet despite this progress, there are still a number of uncertainties particularly in relation to changes in environmental conditions in grain silos, notably those due to temperature and moisture as well as those due to unpredictable flow patterns. The latter often arises in the case of tall silos and in silos with multi or eccentric outlets.

The purpose of this paper is to present an overview of the present state of knowledge associated with silo design for the safe storage of bulk granular materials. The factors influencing the loads in the walls of silos are many and varied and, as is often the case, the loads are a combination of several interacting effects. The paper, focuses on silo wall loads indicating how these are influenced by the discharge flow pattern. The complexity of loading patterns due to eccentric and multiple outlets is mentioned. The effects of moisture content on grain swelling is discussed with particular reference to the significant increase in silo wall loads that may occur. In addition, the influence on wall loads of pressures due to aeration and thermal expansion and contraction of silos is indicated. The use of anti-dynamic tubes to control the wall pressures during discharge of grain in tall single and multi-outlet silos is outlined. Finally the phenomenon of 'silo quaking', a term used to describe pulsating loads which may be experienced during discharge is discussed. If the frequency of the flow pulsations is in harmony with any of the natural frequencies of the structure, severe dynamic loads and stresses can occur. The various mechanisms of 'silo quaking' are outlined and methodologies to determine the magnitude and distributions of the dynamic loads is given.

Handling Plant Design—Basic Concepts

As background information to the study of grain storage and handling, the basic concepts of handling plant design for the general class of bulk materials is briefly reviewed.

General remarks

The procedures for the design of handling plant, such as storage bins and silos, feeders and chutes are well established and follow the four basic steps:

* Institute for Bulk Materials Handling Research, The University of Newcastle, NSW 2038, Australia

(i) Determination of the strength and flow properties of the bulk solids for the worst likely flow conditions expected to occur in practice.
(ii) Determination of the bin, stockpile, feeder or chute geometry to give the desired capacity, to provide a flow pattern with acceptable characteristics and to ensure that discharge is reliable and predictable
(iii) Estimation of the loadings on the bin and hopper walls and on the feeders and chutes under operating conditions.
(iv) Design and detailing of the handling plant including the structure and equipment.

The general theory pertaining to gravity flow of bulk solids and associated design procedures are fully documented (Jenike 1961, 1964; Arnold 1982; Roberts 1988). For the purpose of the present discussion, the salient aspects of the general philosophy are briefly reviewed.

Modes of flow in bins and silos of symmetrical geometry.

Following the definition by Jenike (Jenike 1961, 1964) the two principal modes of flow are mass-flow and funnel-flow. These are illustrated in Figure 1.

In mass-flow, the bulk solid is in motion at every point within the bin whenever material is drawn from the outlet. There is flow of bulk solid along the walls of the cylinder (the upper parallel section of the bin) and the hopper (the lower tapered section of the bin). Mass-flow guarantees complete discharge of the bin contents at predictable flow rates. It is a 'first-in, first-out' flow pattern; when properly designed, a mass-flow bin can re-mix the bulk solid during discharge should the solid become segregated upon filling of the bin. Mass-flow requires steep, smooth hopper surfaces and no abrupt transitions or in-flowing valleys.

Mass-flow bins are classified according to the hopper shape and associated flow pattern. The two main hopper types are conical hoppers which operate with axi-symmetric flow and wedged-shaped or chisel-shaped hoppers in which plane-flow occurs. In plane-flow bins, the hopper half-angle α will usually be, on average, approximately 8° to 10° larger than the corresponding value for axi-symmetric bins with conical hoppers. Therefore, they offer larger storage capacity for the same head room than the axi-symmetric bin, but this advantage is somewhat offset by the long slotted opening which can give rise to feeding problems. The transition hopper, which has plane-flow sides and conical ends, offers a more acceptable opening slot length. Pyramid shaped hoppers, while simple to manufacture, are undesirable in view of build-up of material that is likely to occur in the sharp corners or in-flowing valleys. This may be overcome by fitting triangular-shaped gusset plates in the valleys.

Funnel-flow occurs when the hopper is not steeply sloped and the walls of the hopper are not smooth enough. In this case, the bulk solid sloughs off the top surface and falls through the vertical flow channel that forms above the opening. Flow is generally erratic and gives rise to segregation problems. In the case of cohesive bulk solids, flow will continue until the level of the bulk solid in the bin drops an amount H_D equal to the draw-down. At this level, the bulk strength of the contained material is sufficient to sustain a stable rathole of diameter D_f as illustrated in Figure 1b. Once the level defined by H_D is reached, there is no further flow and the material below this level represents 'dead' storage. This is a major disadvantage of funnel-flow. For complete discharge, the bin opening needs to be at least equal to the critical rathole dimension determined at the bottom of the bin corresponding to the bulk strength at this level. However, for many cohesive bulk solids and for the normal consolidation heads occurring in practice, ratholes measuring several metres are often determined. This makes funnel-flow impracticable. Funnel-flow has the advantage of providing wear protection of the bin walls, since the material flows against stationary material. However it is a 'first-in last-out' flow pattern which is unsatisfactory for bulk solids that degrade with time. It is also unsatisfactory for fine bulk solids of low permeability. Such materials may aerate during discharge through the flow channel and this can give rise to flooding problems or uncontrolled discharge.

In the case of cohesive bulk solids, the disadvantages of funnel-flow may be overcome by the use of expanded-flow, as illustrated in Figure 2. This combines the wall protection of funnel-flow with the reliable discharge of mass-flow. Expanded-flow is ideal where large tonnages of bulk solid are

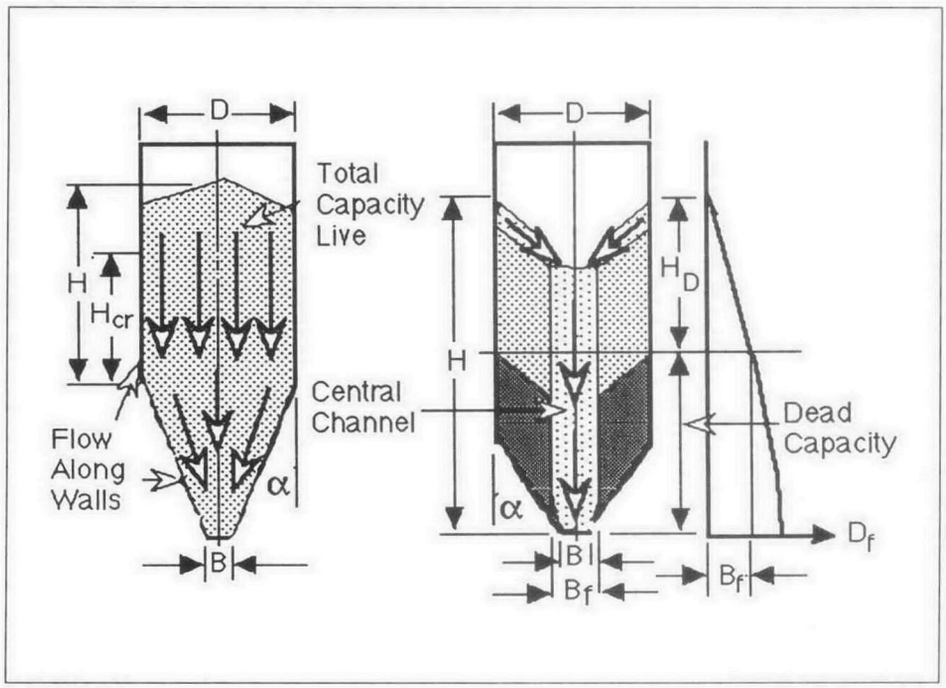

Fig. 1 Modes of flow (a) Mass-flow; (b) Funnel-flow

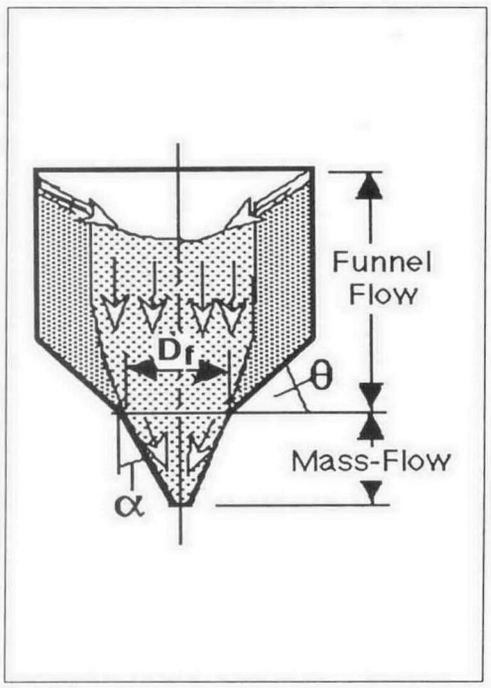

Fig. 2. Expanded flow

to be stored. For complete discharge, the dimension at the transition of the funnel-flow and mass-flow sections must be at least equal to the critical rathole dimension at that level. Expanded-flow bins are particularly suitable for storing large quantities of bulk solids while maintaining acceptable head heights. The concept of expanded-flow may be used to advantage in the case of bins or bunkers with multiple outlets.

Generally speaking, symmetric bin shapes provide the best performance. Asymmetric shapes often lead to segregation problems with free flowing materials of different particle sizes and makes the prediction of wall loads very much more difficult.

Free-flowing granular materials

Since most bulk grains at low moisture contents are generally free flowing, they have no bulk strength. Hence funnel flow, as illustrated in Figure 3, is a viable option. During discharge, an 'effective transition' (ET) forms and this defines the lower region of the flow channel during discharge. Once the head drops during the last stages of discharge, the grain will eventually settle at its final repose angle as indicated as indicated in Figure 3a. However, the grain retained in the 'dead' region of the silo may degrade with time and contaminate fresh grain loaded into the silo. For this region, the silo should be self emptying, which may be accomplished by using a hopper bottom as illustrated in Figure 3b.

Even though funnel-flow silos may be used to store and handle grain, the disadvantages of a 'first-in, last-out' flow pattern which could lead to a reduction in grain quality, needs to be noted. For this reason, the advantages of mass-flow should not be overlooked even though a steeper hopper is required as in Figure 1a. Certainly, if the grain is at a higher moisture content, it will exhibit cohesive strength. In this case mass-flow is definitely the preferred option.

Mass-flow and funnel-flow limits for symmetrical bins

Established theory due to Jenike

The mass-flow and funnel-flow limits have been defined by Jenike on the assumption that a radial stress field exists in the hopper (Jenike 1961, 1964). These limits are well known and have been used extensively and successfully in bin and silo design. The limits for axi-symmetric or conical hoppers and hoppers of plane-symmetry depend on the hopper half-angle α, the effective angle of internal friction δ and the wall friction angle ϕ. Once the wall friction angle and effective angle of internal friction have been determined by laboratory tests, the hopper half-angle may be determined. The bounds for conical and plane-flow hoppers are plotted for three values of δ in Figure 4. In functional form,

$$\alpha = f(\phi,\delta) \qquad (1)$$

In the case of conical or axi-symmetric hoppers, it is recommended that the half-angle be chosen to be 3° less than the limiting value. For plane-flow, the bounds between mass and funnel-flow are much less critical than for conical hoppers. In plane-flow hoppers, much larger hopper half angles are possible which means that the discharging bulk solid will undergo a significant change in direction as it moves from the cylinder to the hopper. For plane-flow, the design limit may be selected; if the transition of the hopper and cylinder is sufficiently radiused so that the possibility for material to build-up by adhesion is significantly reduced, then a half-angle 3° to 4° larger than the limit may be chosen.

Typically for wheat, average values of the friction angles are δ = 30°, ϕ = 20° for polished stainless steel or polished mild steel and ϕ = 25° for mild steel plate as rolled. For mass-flow in conical or axi-symmetric hoppers, the required hopper half-angles (Figure 1(a)) are α_c = 25° for the polished surfaces and α_c = 17° for the rolled mild steel. In the case of plane-flow, wedged-shaped mass-flow hoppers, the corresponding angles are α_p = 35° and α_p = 27° respectively.

Modification to mass-flow limits—more recent research

Since in the work of Jenike, flow in a hopper is based on the radial stress field theory, no account is taken of the influence of the surcharge head due to the cylinder on the flow pattern developed, particularly in the region of the transition. It is been known for some time that complete mass-flow in a hopper is influenced by the cylinder surcharge head. For instance, there is a minimum level H_{cr} which is required to enforce mass-flow in the hopper (Thompson 1984). For the mass-flow bin of Figure 1a, this height ranges from approximately 0.75 D to 1.0 D.

More recent research has shown that the mass-flow and funnel-flow limits require further explanation and refinement. For instance, Jenike published a new theory to improve the prediction of funnel-flow; this led to new limits for funnel-flow which give rise to larger values of the hopper half-angle than previously predicted, particularly for high values of the wall friction angle. In the earlier theory, the boundary between mass-flow and funnel-flow was based on the condition that the

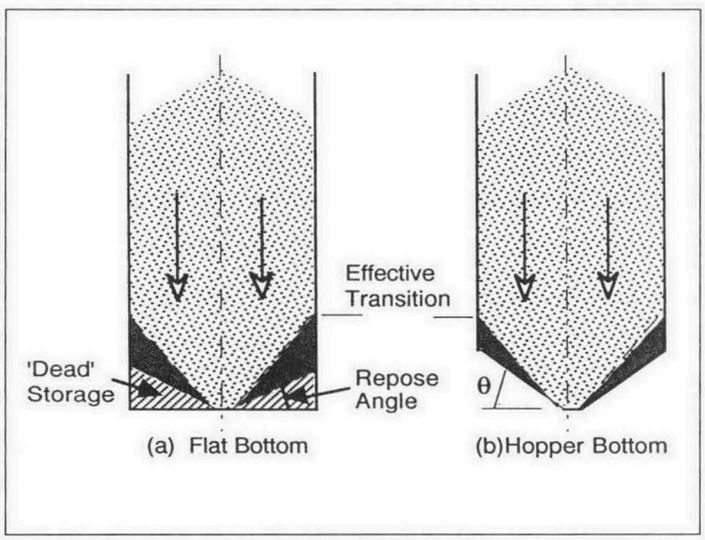

Fig. 3. Funnel-flow for free-flowing granular material

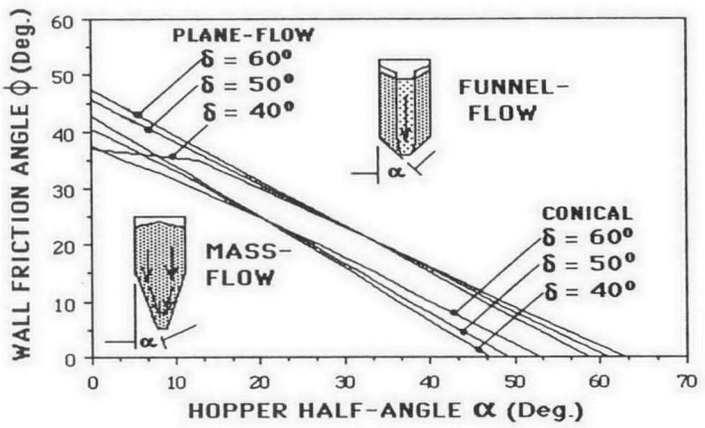

Fig. 4 Limits for mass-flow for conical and plane-flow channels

stresses along the centre line of the hopper became zero. In the revised theory the flow boundary is based on the condition that the velocity becomes zero at the wall.

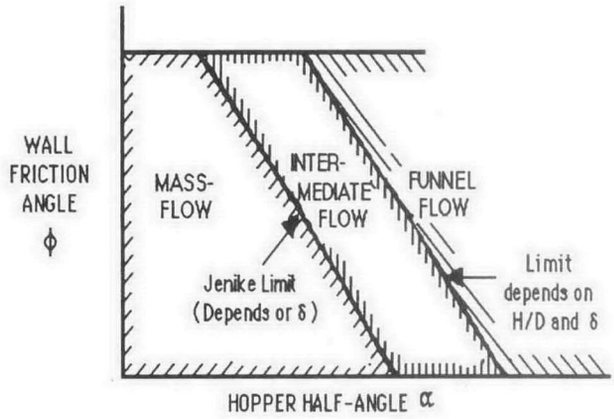

Fig. 5. Flow regimes for plane-flow hopper defined by Benink (1989)

In a comprehensive study of flow in silos, Benink (1989) has identified three flow regimes, mass-flow, funnel-flow and an intermediate flow as illustrated in Figure 5. Whereas the radial stress theory ignores the surcharge head, Benink has shown that the surcharge head has a significant influence on the flow pattern generated. He derived a fundamental relationship for H_{cr} in terms of the various bulk solid and hopper geometrical parameters, notably the H:D ratio of the cylinder and the effective angle of internal friction δ. Benink developed a new theory, namely the 'arc theory', to quantify the boundaries for the three flow regimes. This theory predicts the critical height H_{cr} at which the flow changes.

Intermediate-flow is illustrated in Figure 6. Grain flows more quickly in the central flow channel. The nature of the flow is such that pulsating loads may be induced. The characteristics of pulsating dynamic loads is discussed in Section 8.

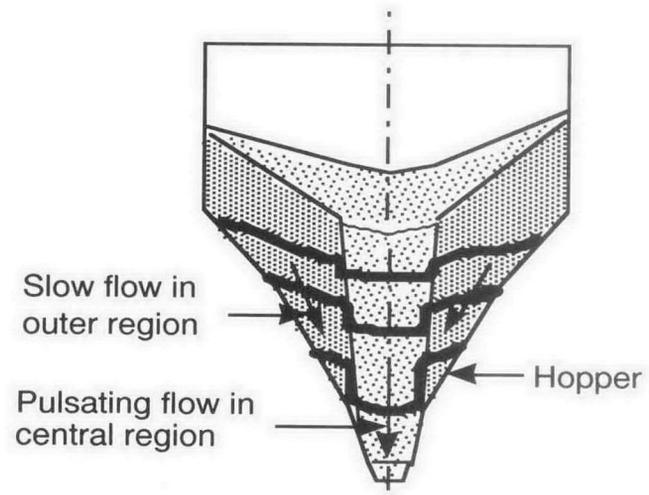

Fig. 6. Intermediate flow illustrating pulsating flow regime.

Hopper opening dimension for mass-flow

The principles embodied in mass-flow hopper design are illustrated in Figure 7. Having selected the basic shape, that is, whether the hopper is to be axi-symmetric (conical) or plane-flow (wedge-shaped), the hopper half angle α is determined on the basis of the wall friction angle ϕ. It then remains to determine the required dimension of the channel to ensure that arching does not occur and the required flow rate is achieved. In most cases, the critical dimension for flow occurs at the outlet.

The parameter used to describe the strength of a bulk solid is the Flow Function which is abbreviated as '*FF*'. The *FF* represents the variation of the unconfined yield strength σ_c as a function of the major consolidation pressure σ_1 and is illustrated in Figure 7a. For free-flowing grain, $\sigma_c = 0$ and the FF graph coincides with the horizontal axis. Referring to Figure 7b, the stress acting in the arch is represented by $\overline{\sigma}_1$ and is related to the major consolidation pressure σ_1 by the 'flow factor' ff, a flow channel parameter, as follows:

$$\overline{\sigma}_1 = \frac{\sigma_1}{ff} \qquad (2)$$

For the critical condition, the minimum opening dimension B occurs when $-\sigma_1 = \sigma_c$ and is given by

$$B_{\min} = \frac{\overline{\sigma}_1 H(\alpha)}{\rho g} \qquad (3)$$

where $H(\alpha)$ = Arch thickness and hopper geometry factor parameter based on Hopper Half Angle (Jenije 1961, 1964; Arnold 1982; Roberts 1988).

ρ = Bulk Density

g = acceleration due to gravity

In practice, the actual opening dimension B is made larger than B_{min} in order to achieve the desired flow rate. For the enlarged opening, the actual Flow Factor ff_a applies and the major consolidating pressure at the outlet increases to the value corresponding to the actual opening dimension B.

Silo Wall Loads

In bin and silo design, the prediction of wall loads continues to be a subject of some considerable complexity. In view of its obvious importance it is a subject that has attracted a good deal of research effort. A brief selection of published research which deals with the subject of wall pressures is given in Arnold (1982); Roberts and Ooms (1983); Ooms and Roberts (1985); Roberts (1988a,b); Rombach and Eibl (1989); Ooi and Rotter (1989); and Wu (1990).

Despite the widely varying approaches to the analysis of bin wall loads, it is clear that the loads are directly related to the flow pattern developed in the bin or silo. The flow pattern which a mass-flow bin exhibits is reasonably easy to predict and is reproducible. However, in funnel-flow bins the flow pattern is more difficult to ascertain, especially if the bin has multiple outlet points, the loading of the bin is not central and/or the bulk solid is prone to segregation. Unless there are compelling reasons to do otherwise, bin shapes should be kept simple and symmetric.

The subject of bin loads has been addressed in several design codes notably the recent Australian Standard AS3774-1990, 'Loads on Bulk Solids Containers' (SAA 1990). The earlier codes concentrated on funnel-flow bins, but the later codes cover both mass-flow and funnel-flow bins. In particular, AS 3774-1990, is very comprehensive in the range of loading conditions included and in the types of bins considered.

Symmetric mass-flow bins

The stress fields and normal wall pressures occurring in mass-flow bins for the initial filling and flow conditions are shown in Figure 8. When a bin is initially filled from the empty condition, a peaked stress field occurs as in Figure 8a; the

major principal pressure is almost vertical. When flow occurs, the stress field in the hopper switches to an arch stress field, the switch travelling up the hopper becoming locked in at the transition as in Figure 8b. In the arched stress field, the load is transmitted to the wall of the hopper with the major principal stress acting more in a horizontal direction.

Above the hopper, that is in the cylinder, the peaked stress field remains, although imperfections in the cylinder wall which give rise to localised flow convergences cause over-pressures to occur in the cylinder. Imperfections in bin walls, which give rise to over-pressures, may be due to manufacturing and/or constructional details such as weld projections or plate shrinkages in the case of steel bins or deformation of form work in the case of concrete bins. Jenike has used strain-energy methods to analyse these over-pressures during flow in the cylinder. In view of the difficulty of using the Jenike strain energy method, design codes generally employ over-pressure factors to account for flow conditions in the cylinder. This is indicated by the upper bound p_n curve for the cylinder in Figure 8b.

It is to be noted that when the bin discharges and the flow is stopped, the stress fields and corresponding pressures shown in Figure 8b will remain. The stress field does not revert to that of Figure 8a; this only occurs if the bin is completely emptied and then filled again.

Wall pressures in symmetric funnel-flow bins

In the case of symmetrical funnel-flow bins or silos, the effective transition previously defined, controls the flow channel in the lower region of the bin as indicated in Figure 9. Above the effective transition the flow occurs along the walls similar to that occurring in a tall mass-flow bin. An over-pressure occurs at the effective transition similar to the switch

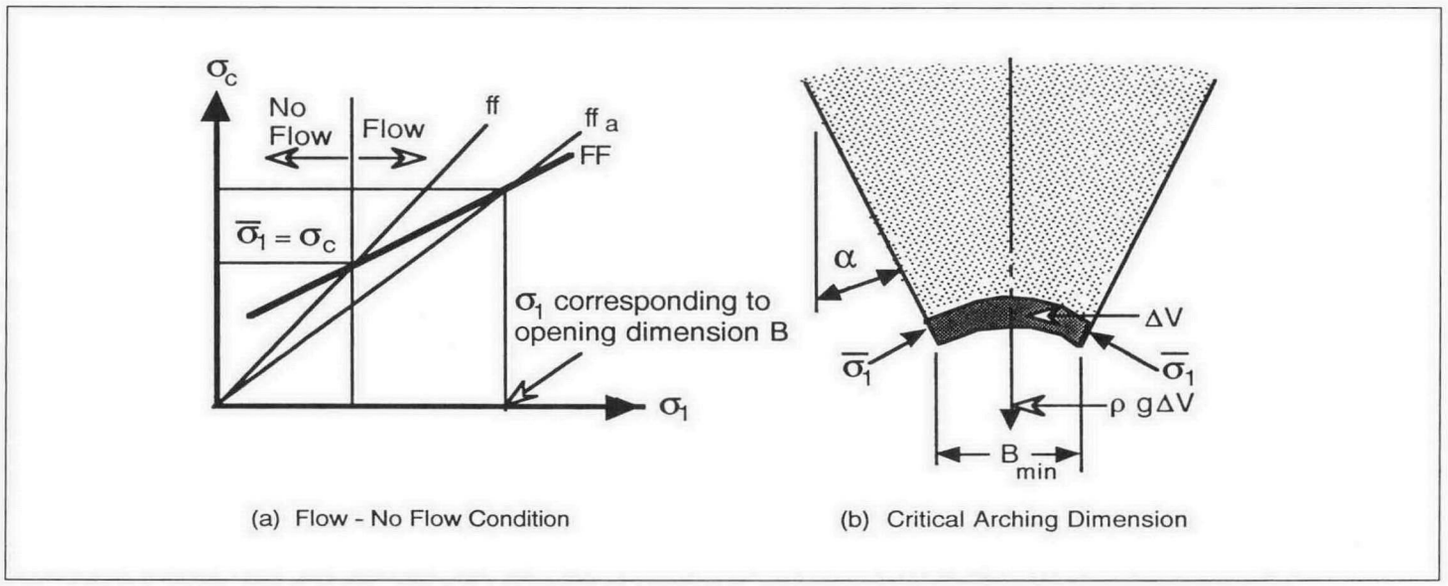

Fig. 7. Determination hopper opening dimension for mass-flow.

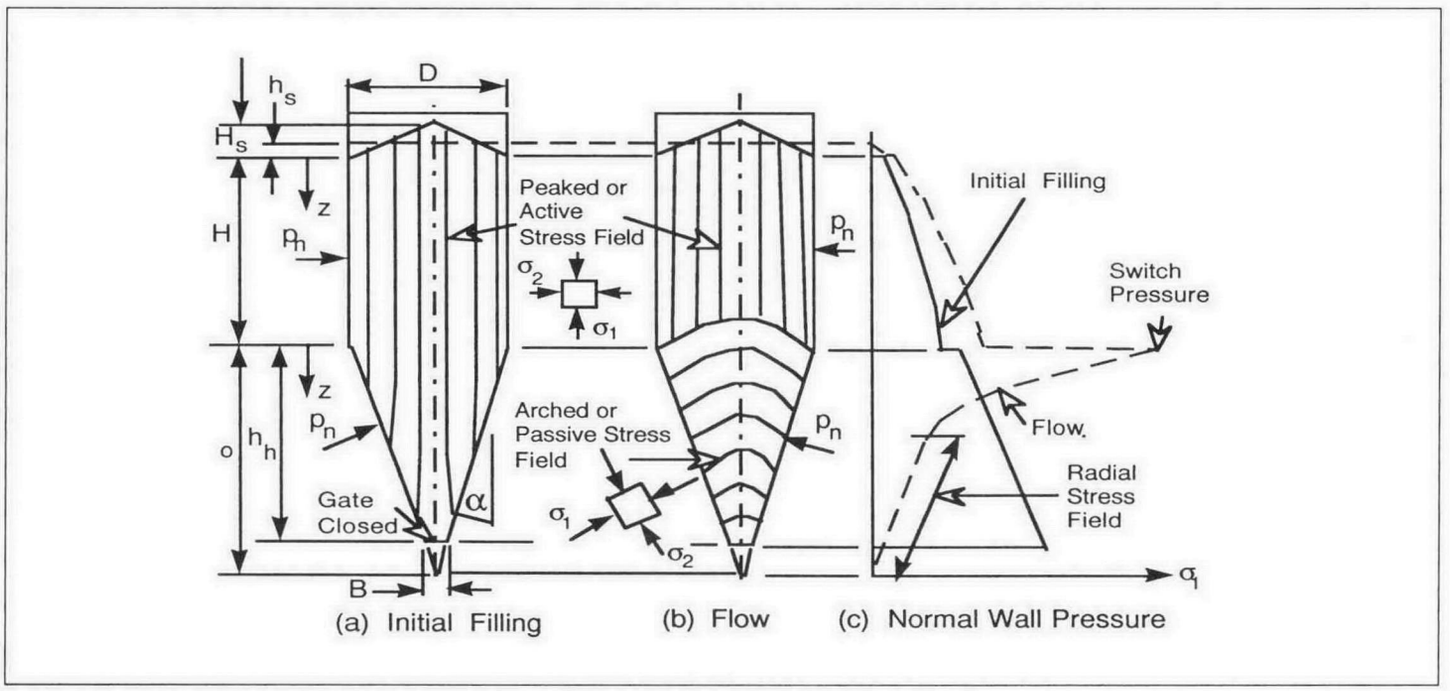

Fig. 8. Pressures acting in mass-flow bins.

pressure in mass-flow, although the magnitude, whilst significant, may not be as severe as the mass-flow switch pressure. Since the effective transition is not stationary but tends to move during the discharge process, the procedure for design involves defining the lowest position at which the effective transition is likely to occur. In the upper cylindrical section of the bin above the effective transition, imperfections in the walls can give rise to increased pressures. The flow pressures in funnel-flow bins, depicted in Figure 9, are normally computed by the application of over-pressure factors on Janssen. The procedures are given in AS 3774 (SAA 1990).

Multiple outlet bins and silos and with eccentric discharge silos

Multiple outlet silos and silos with an eccentric discharge point give rise to complex loading patterns as a result of the flow channels that develop above the outlets. Referring to Figure 10, the pressures acting on the wall in the region of the outlet are of lower magnitude than the pressures that act in the section of the bin or silo where there is no flow. Consequently bending moments are induced in the walls leading to a distortion of the silo's symmetrical cylindrical shape. Apart from the bending stresses which are superimposed on the average hoop stresses at each location, the distorted shape of the silo may give rise to buckling problems.

The subject of eccentric loads in silos is addressed in a comprehensive way in AS3774 (SAA 1990). The loading patterns illustrated in Figure 10 are based on this Standard. It is to be noted that where there are several symmetrically located outlets, the conservative approach to design is to assume that the possibility exists for only one of the outlets to operate at a particular instant.

Moisture Variations in Grain

Free expansion due to moisture increase

Grain, such as wheat, when subjected to increases in moisture, if not completely constrained, will undergo an increase in volume. Changes in moisture content can occur during aeration of grain in bulk storage when the humidity of the circulating air increases. The amount of grain swelling is illustrated in Table 1. This shows the effects of wheat grains after prolonged exposure to high humidity conditions, the results being based on samples conditioned in a humidity cabinet. As indicated the moisture content increased from 9.54% to 20.07% after 4 days, the corresponding increase in volume due to swelling being 17.8%. For moisture changes of lower order the degree of swelling is correspondingly lower.

Constrained expansion due to moisture increase

In a storage bin situation the volume increase due to swelling is constrained. To gauge the possible volume expansion under such constrained conditions, tests were conducted on wheat contained in cylindrical cells with rigid bottoms and side walls with a loaded piston being located on the top of the contained samples, the pistons being free to move in the vertical direction. The moisture content of the grain in the various cells was varied and movement of the piston due to swelling of the grain over varying periods was noted. A typical set of results is shown in Figure 11 which applies to a pressure of 28 kPa. The results indicate, for example, that an increase of moisture content from 9% to approximately 23%, the corresponding expansion of the bulk grain is 1.2%. Under normal conditions of storage moisture variations of this magnitude are unlikely. However the results indicate the order of swelling that may occur during constrained storage; on the basis of such results the increased loading on the walls of silos may be estimated.

Loads in Grain Silos due to Grain Moisture Increase

Possible loading conditions

The loading conditions that may occur are shown in Figures 12 and 13. When grain is subject to swelling, it tends to expand upward as well as outward, the upward movement being resisted by wall friction. In the limiting condition the wall friction acts downward as indicated in Figure 13. The wall friction may not be fully mobilised and the resistance at the wall to upward expansion may be less than for the limiting condition.

Assuming the pressure is uniform across the cross-section, the following differential equation arises

$$\frac{dp_n}{dz} \pm \frac{4\mu K_j}{D} p_n = \gamma K_j \qquad (4)$$

where

+sign applies to the Janssen case of Figure 12

–sign applies to the swelling case of Figure 13

μ= coefficient of friction as the wall

p_V= vertical pressure

p_n= lateral pressure

D= silo diameter

γ= bulk specific weight of wheat

Table 1 Free expansion of humidified wheat

Sample	Storage time (hours)	Moisture content (w.b.)		Volume increase (%)
		Initial (%)	Final (%)	
1	1.0	6.32	7.38	0.62
2	3.75	4.91	8.65	4.74
3	5.0	10.83	13.83	6.05
4	24.0	11.16	16.58	14.52
5	29.0	9.51	19.26	16.40
6	95.0	9.54	20.07	17.79

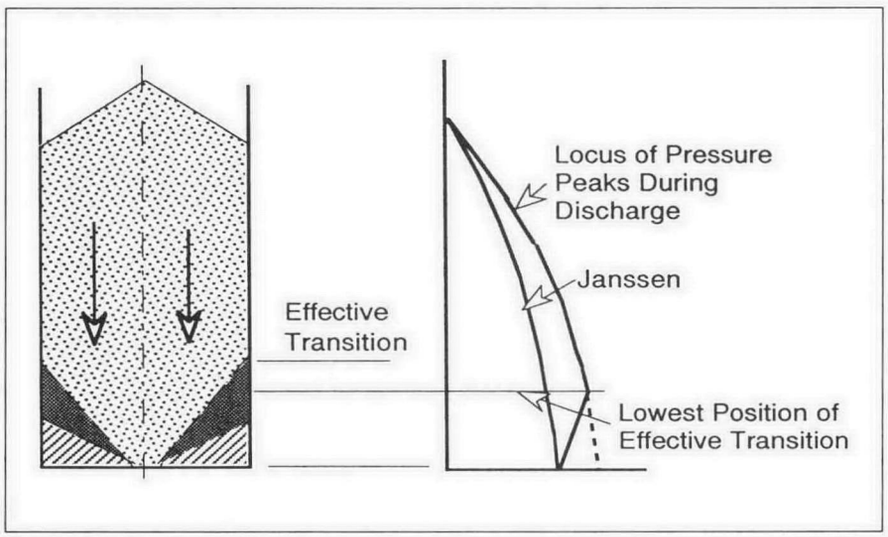

Fig. 9. Pressures in funnel flow silo.

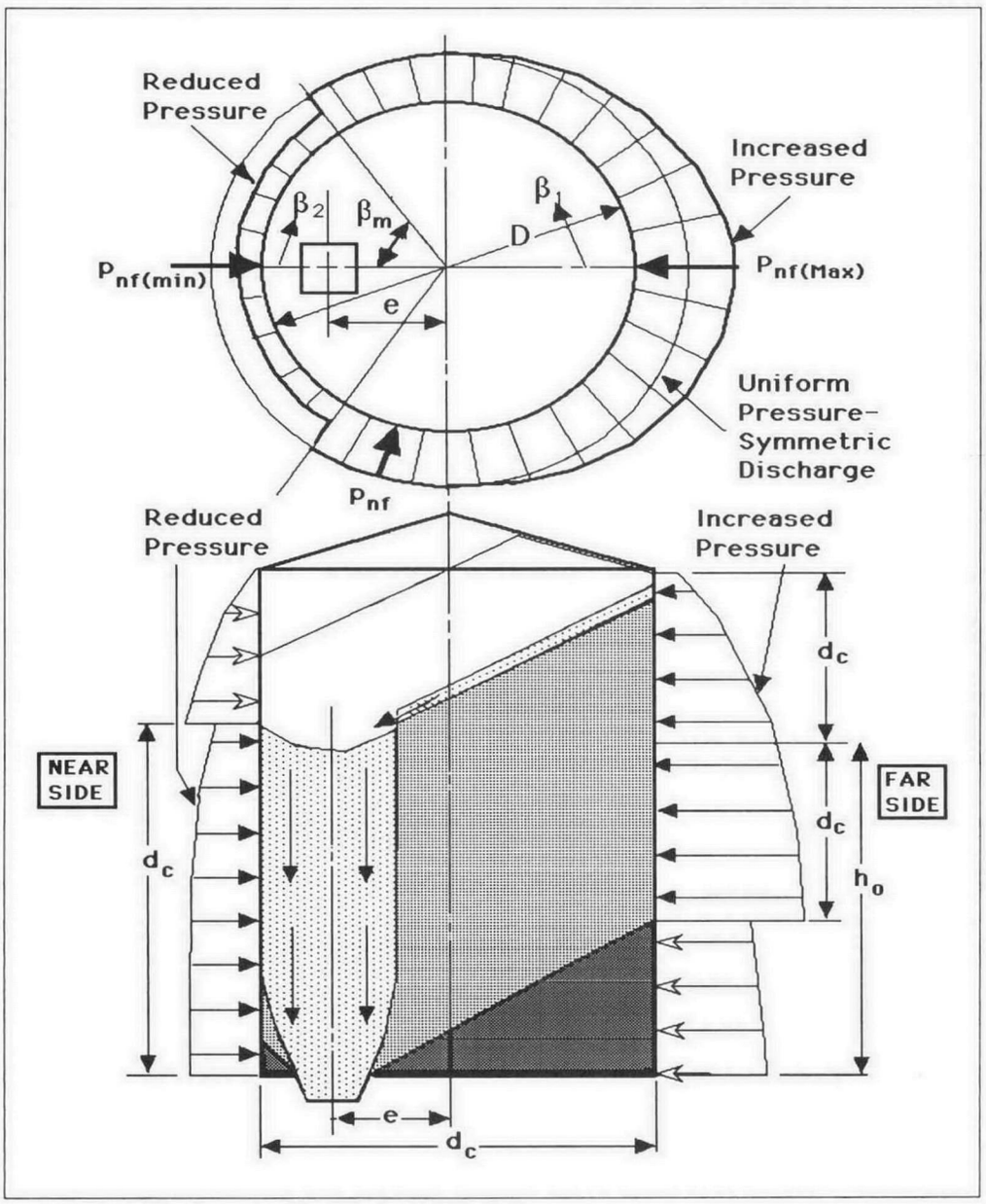

Fig. 10. Circumferential pressure variation due to operation of one eccentric outlet.

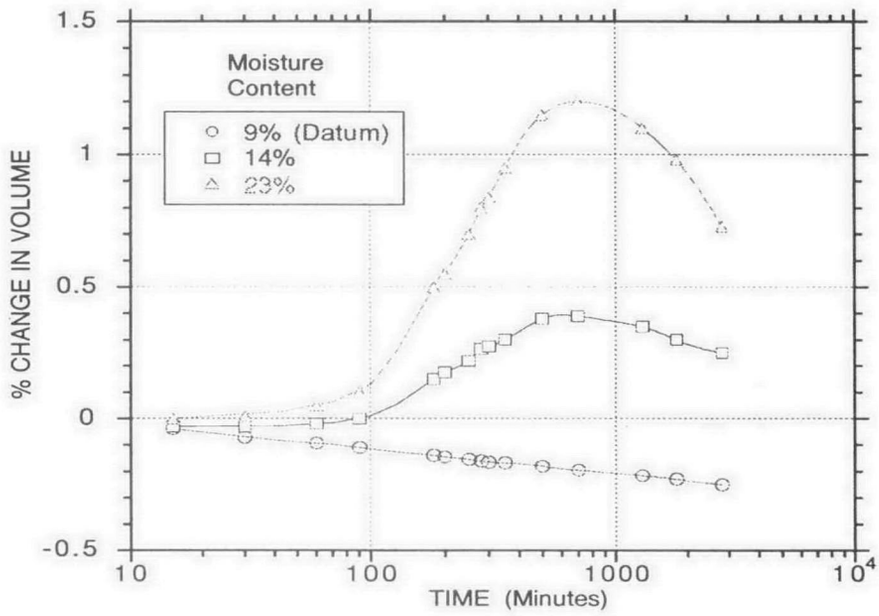

Fig. 11. Expansion of wheat due to swelling under constrained storage pressure applied: 28 kPa.

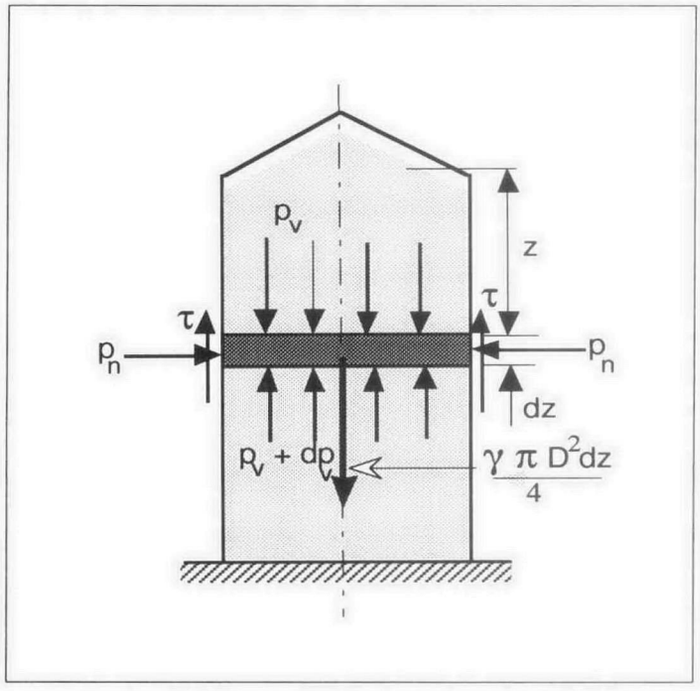

Fig. 12. Janssen pressure due to static loading.

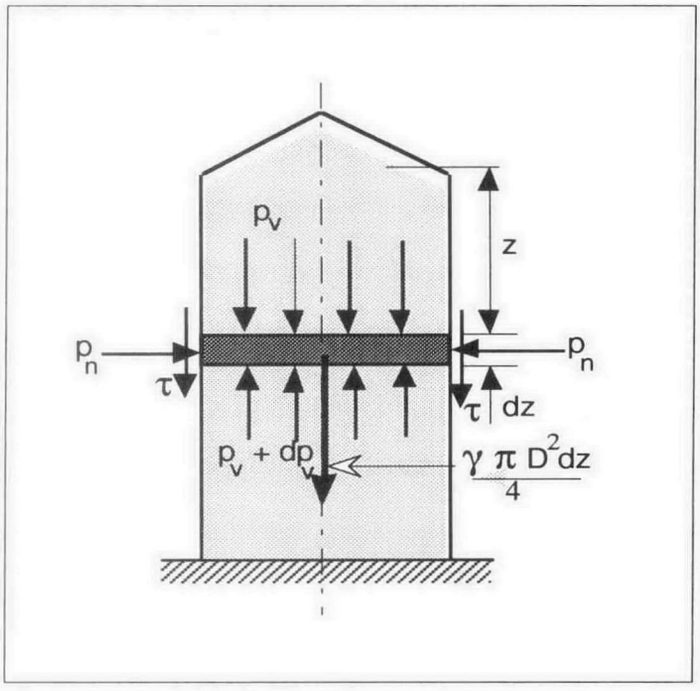

Fig. 13. Effect of upward swelling producing reverse friction forces at wall

Janssen Equation

Putting the + sign into (4) and solving yields the Janssen equation

$$p_n = \frac{\gamma D}{4\mu}\left(1 - e^{-4\mu K_j z/D}\right) \quad (5)$$

and

$$p_v = \frac{p_n}{K_j} \quad (6)$$

For silo design, where the loading is symmetrical, it is usual to apply an over-pressure factor to the pressure p_n of equation (5).

'Piston' equation for grain swelling

Grain swelling may occur if moist air is circulated through stored grain via aeration ducts as illustrated in Figure 14. Physically the effect of grain swelling is likened to a piston trying to push the column of grain upward (Roberts 1988). Putting the minus sign into equation (4) and solving yields

$$P_n = \frac{\gamma D}{4\mu}\left(e^{4\mu K_j z/D} - 1\right) \quad (7)$$

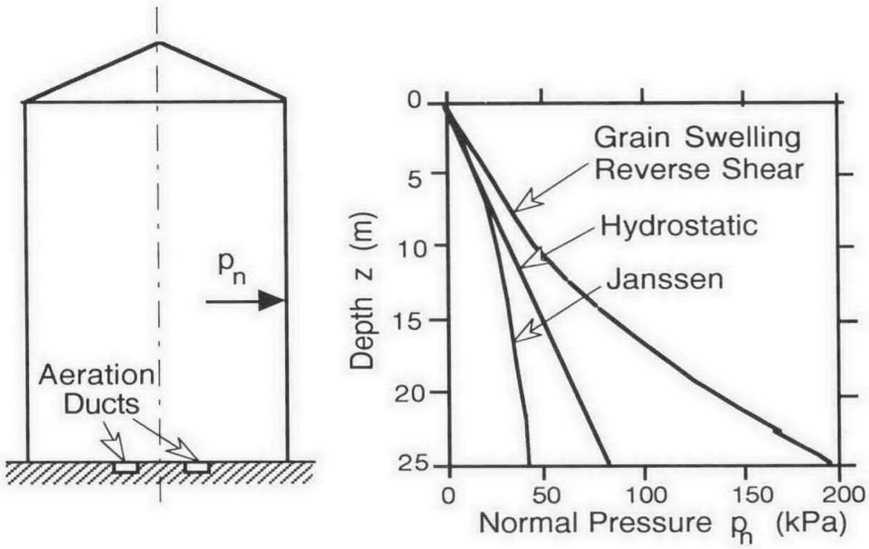

Fig. 14. Wall pressure distributions in 15 m diameter by 25 m high wheat silo.

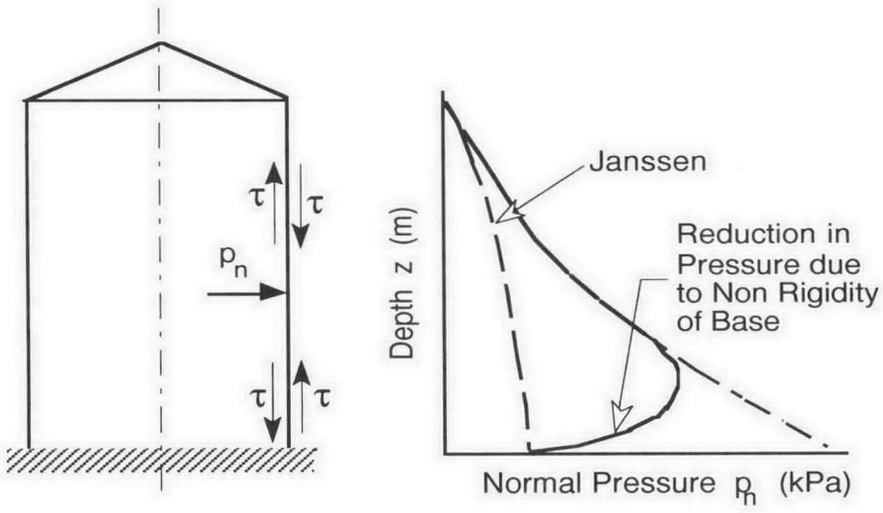

Fig. 15. Reduction in wall pressures in lower region of silo walls.

Equation (7) assumes the wall friction is fully mobilised. An intermediate case of interest occurs when the wall resistance reduces to zero which implies that the vertical wall support just equals the upward force at the wall due to swelling. In this case the vertical pressure p_V is equal to the hydrostatic pressure

$$p_V = \gamma z \quad (8)$$

and $$p_n = K_j \gamma z \quad (9)$$

The graphs depicting the wall pressures, based on equations (5), (7) and (8) are shown In Figure 14.

The large magnitude of the pressures given by equation (7) other than for the Janssen pressure given by equation (5) is clearly evident. The pressure curves in Figure 14 apply to a 15 m diameter by 25 m tall wheat silo and have been plotted for a constant value of $K_j = 0.4$. It is possible that K_j will be higher for the grain swelling case, increasing the pressures beyond those plotted.

Some general comments

There seems no doubt that an increase in moisture content of the grain can cause a significant increase in the silo wall pressures. The key to this behaviour is the direction and magnitude of the friction force at the wall. When the friction force acts downward, a 'piston effect' is produced in the silo where the forces in the silo wall resisting upward expansion of the grain can become quite considerable. This would be particularly the case for tall silos where the height is several times the diameter.

The extent to which the frictional forces at the wall change in magnitude and direction over the full height of the silo are virtually impossible to predict. If the floor of the silo is not entirely rigid, then the frictional forces in the wall in the lower region of the silo would act upward and the pressures exerted on the silo walls in this region would reduce. This is depicted in Figure 15.

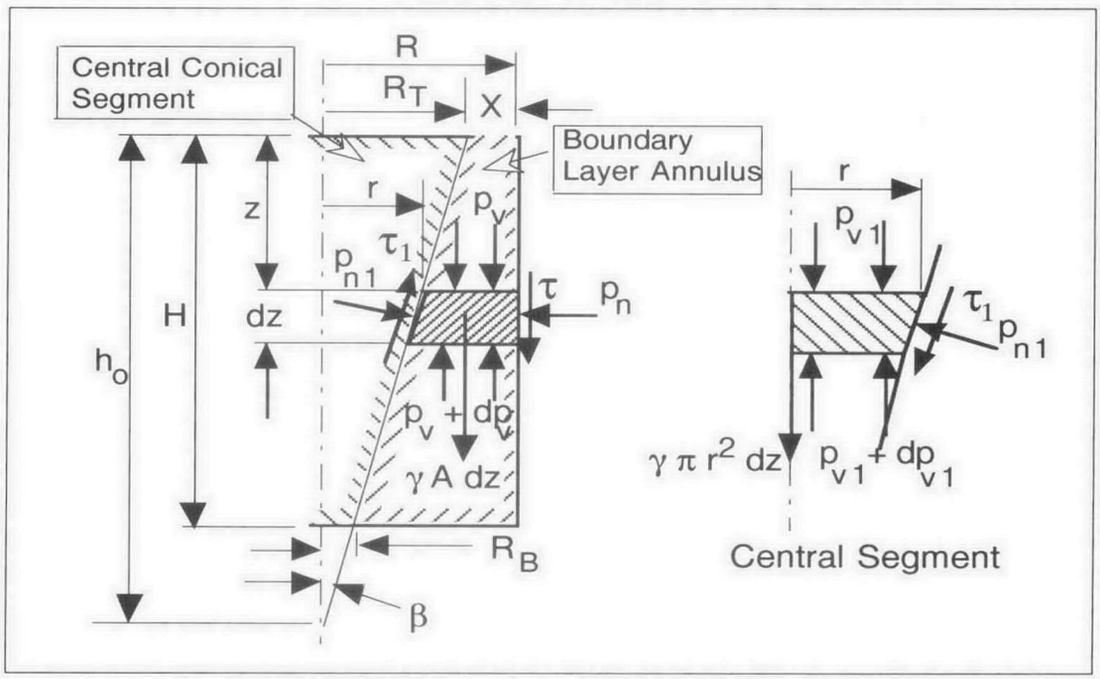

Fig. 16. Silo pressure model showing boundary layer annulus to account for grain swelling.

Simplified theory for estimating silo wall pressures due to grain swelling

It is evident that the large size of actual silos would be such that pressure distribution at any cross section would not be uniform. Furthermore, there is every reason to believe that the moisture content of the stored grain would not be uniformly distributed throughout the mass; the geometry and location of the air supply ducts suggest this would be the case.

In reality the behaviour of the grain during swelling is likely to produce a boundary layer effect. The model used by Roberts (1988a,b) to analyse this case is illustrated in Figure 16. A conical rupture surface is assumed, this surface being sloped at an angle β to the vertical and intersecting the top surface of the silo at a radius R_T. It is assumed that the conical central portion of the grain mass is able to expand upwardly due to grain swelling and induce pressures in the outer, wedge-shaped annulus comprising the boundary layer. The outer boundary layer annulus is constrained by the silo walls; as the thickness of this annulus increases, the greater become the proportion of the grain mass which must be constrained by the silo walls and hence the greater become the pressures on the walls.

The differential equations for the grain pressures have been derived and numerical solutions obtained(Roberts 1988a). The silo in this case is 15 m diameter by 25 m high and stores wheat. Some typical results for various R_B/R_T ratios and various values of X (Figure 16) being shown in Figure 17. As indicated, the presence of the boundary annulus significantly influences the wall pressures. In general, as the dimension X increases, then the closer does the pressure distribution approach that depicted in Figure 14, and the greater becomes the pressure. For comparison purposes the Janssen curve and the pressure curve for reverse friction or shear of Figure 14 are also included in Figure 17.

The change in pressure with change in dimension X are shown more clearly in Figure 18. At the base of the silo, that is at z = 25 m, the pressure increases quite significantly as X increases. At the depth z = 20 m the increase in pressure is less pronounced, while at the depth z = 10 m, there is little variation in pressure with increase in X. Based on the assumptions

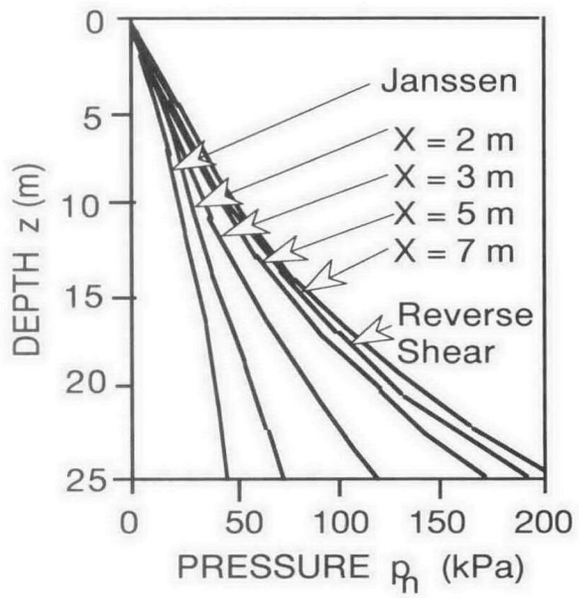

Fig. 17. Influence of boundary layer on silo wall. Pressure distributions, $R_B/R_T = 0.5$.

made in the foregoing analysis, the results indicate that the maximum pressure at the base of the silo with zero boundary layer is close to 200 kPa. With the presence of a boundary layer the pressures acting at the wall are reduced considerably. The peak pressure with zero boundary layer is 4.2 times the Janssen pressure while with a boundary layer thickness of say X = 2 m, the wall pressure at the base of the silo is approximately 1.5 times the Janssen pressure. These values are based on the pressure ratio K = 0.4 and R_B/R_T = 0.5. It is to be noted that based on experiments to examine grain swelling, and allowing for the relative elasticity of the wheat and the steel silo shell, the estimated increase in pressure is of the order of 2 to 1.

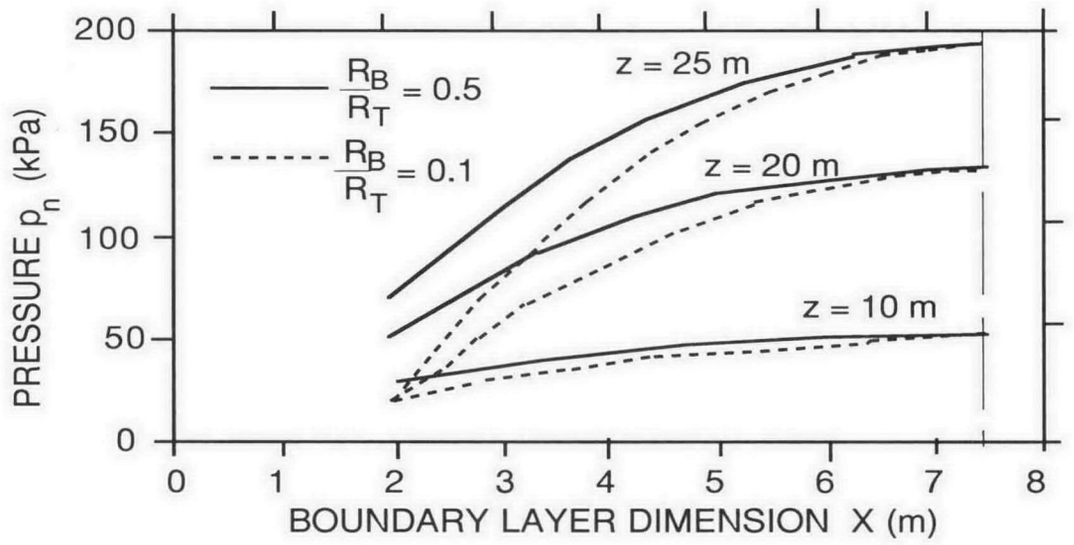

Fig. 18. Variation of silo wall pressures with boundary layer. Dimension at selected depths.

While the foregoing analysis is an approximation, it does provide an indication of the influence of a boundary layer in tempering the wall pressures generated as a result of grain swelling.

Other Factors Influencing Bin and Silo Loadings

In addition to moisture, other environmental factors may influence bin and silo wall loadings. Two of these factors, namely aeration and temperature effects, are briefly discussed.

Silo aeration— effect of air pressure

Pressures due to aeration must be added to the pressures generated by the bulk material itself. Jenkyn (1978) considered likely packaging configurations during aeration and concluded that body-centred cubes would occur most frequently. These produce a maximum increase in value occupied by the material of approximately 25% with a corresponding decrease in density. Jenkyn recommends a design pressure given by

$$P_{des} = P_h + P_a \tag{10}$$

where

$$P_h = \frac{0.8\gamma D}{4\mu}\left(1 - e^{-4\mu K_o h/D}\right) \tag{11}$$

γ = Bulk specific weight
D = Silo diameter
μ = Coefficient of friction
h = Head
K_O = Lateral pressure coefficient.
Under aeration conditions K_O may approach unity.
The aeration pressure is given by

$$P_a = \frac{\Delta_p h}{h_o} \tag{12}$$

where Δp = Maximum aeration pressure
h_O = Effective maximum material depth.

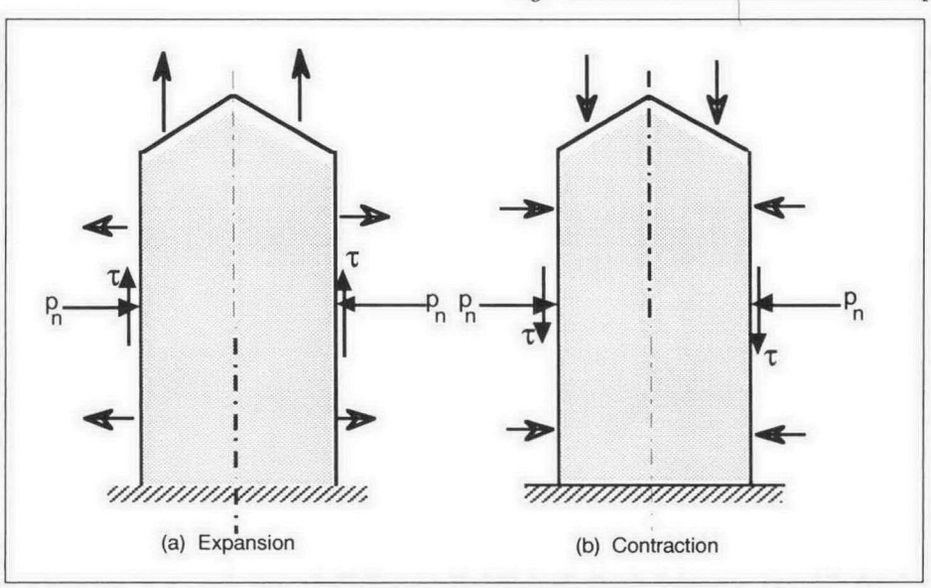

Fig.19. Expansion and contraction of silo.

The foregoing assumes symmetrically located air injection points and a uniform air distribution. In practice, variations in grain packing densities and variations in moisture throughout the bulk grain mass could give rise to non-uniform pressure distributions in eccentric loadings.

Temperature variations

The variations methods use to analyse the wall pressure in steel silos generally assume a rigid silo. This is not the case. Daily, weekly and monthly variations in atmospheric temperatures cause the shell of a silo to expand and contract with some settling of stored material during expansion with little recovery, if any, during contraction. This can be a problem in the case of silos storing bulk materials over long periods of time without discharge.

When the silo expands due to temperature increase, it does so by expanding radially outward and upward. This allows the grain to settle. When the silo contracts it does so by contracting radially inwards and downward, the latter effect causing the friction force at the wall to switch from the initially upward direction to the downward direction, as depicted in Figure 19. This has the effect of significantly increasing the pressure in a similar way to that of increased moisture. Since the temperature cycles on a daily basis, as well as decreasing on a longer-term basis, the combined effect of the progressive settling of the grain and the action of the reversed friction force at the walls could have a most significant influence on the structural safety of the silo.

Measurements of daily temperature fluctuations and pressures generated in walls of steel silos have indicated quite clearly a significant increase in pressures during the night period when temperatures were lower than during the day. Apart from the daily temperature fluctuations, the overall changes from summer to winter can have a significant effect. For example, in a 15 m diameter steel silo, a temperature increase of 20° could cause an expansion in the order of 3 mm. If, hypothetically, the silo contained wheat and was completely rigid so that the contraction of the silo were prevented as the temperature dropped, an increase in wall pressure of 18 kPa would occur, this being 41% of the maximum static wall pressure. However, the elasticity of the wheat relative to steel needs to be taken into account. The modulus of elasticity of wheat varies significantly from one wheat type to another [16]. Based on the properties of individual grains, a typical elasticity modules for wheat is $E_W = 2.07 \times 10^9$ kPa gives

$(E_W/E_S) = 0.01 = 1\%$

Using this ratio, one daily expansion and contraction could produce a residual increase in wall pressure of 0.1 kPa. While this is in itself insignificant, the cumulative effect of expansion and contraction over a period of days and weeks is significant. For example, extrapolation of the data for a two-month period indicates a cumulative increase in pressure of 11 kPa or 25% of the maximum static wall pressure. This is an upper bound value since the modules E_W for bulk wheat is less than that given above. Furthermore the analysis is greatly simplified; the actual process of expansion and contraction coupled with the effect of cyclical loadings on the grain and influence of moisture variations is an extremely complex problem to analyse. However the quoted example indicates the possible order of magnitude of increase in wall pressure due to repeated expansion and contraction.

It must be noted that the foregoing discussion assumes uniform temperatures around the periphery of the silo. This will not occur in practice; there will be differential expansion owing to the position of the sun relative to the silo walls. The loading pattern will be more complex and the resulting pressure changes around the periphery will not be uniform.

Use of Anti-dynamic Tubes to Control Silo Pressures

In tall grain silos, the effective transition occurs low down the silo walls; as a result, mass-flow of grain with flow along the walls occurs over a substantial height of the silo above the effective transition. The effect is to cause dynamic pressures to be generated, these pressures being in the order of two to three times the static pressures generated after the silo is filled from the empty condition.

As shown by Reimbert (see Thompson 1984), it is possible, by the use of an anti-dynamic tube, to control the flow pattern so that funnel-flow always occurs without flow along the walls. In this way, the wall pressures never exceed the static values. Reimbert's anti-dynamic tube, placed centrally in a symmetrical silo, extends almost the whole height and has a series of holes or ports to allow grain to enter the tube at various levels.

A variation of the Reimbert tube is the tremmie tube which has no holes in the walls and extends slightly less than half the height of the silo. Research using this type of anti-dynamic tube was conducted at the University of Newcastle, Australia (Ooms and Roberts 1985; Roberts 1988b). Figure 20 shows, schematically, the 1.2 m diameter by 3.5 m tall model flat bottom test silo and a sample set of test results for the normal wall pressures. Load cells fitted in the wall of the silo enabled these measurements to be taken.

The work was initiated in order to provide a simple and low cost solution to controlling the pressures in a number of badly cracked concrete grain silos approximately ten times the scale. In effect, the tremmie tube divides the tall funnel-flow silo into two squat silos in series. The top half of the silo discharges first followed by the bottom part once the level drops below the top of the tremmie tube and the tube empties. Ports in the bottom of the tube allow grain to flow laterally to the silo outlet.

The design of the bottom ports and tube sizing in relation to the silo outlet dimension are important in order to promote automatic choking of the lateral flow at the bottom until the tube empties. No valves are necessary. The arrangement ensures that at no time does the effective transition intersect the walls of the silo and hence the pressures never exceed the values corresponding to the static or initial filling condition. This is illustrated in the test results of Figure 20.

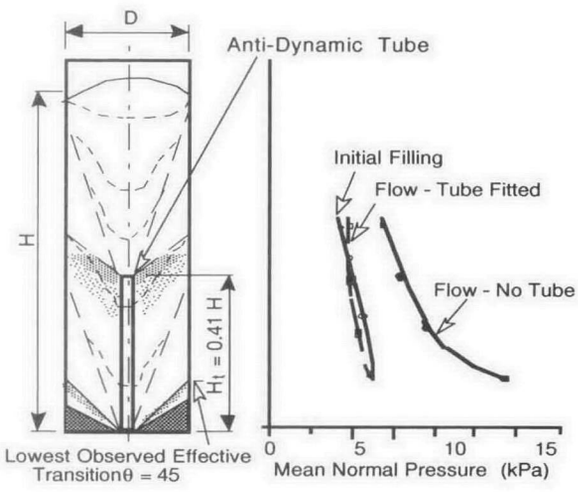

Fig. 20. Model silo studies using anti-dynamic tube.

The anti-dynamic tube described above has been successfully used to control the flow in silos having eccentric and multiple discharge points. Typical applications are shown in Figure 21. Without the tube in place, the walls of such silos are subject to significant bending stresses in addition to the hoop stresses.

It is to be noted that the anti-dynamic tube described here is suitable only for free flowing, cohesionless bulk solids such as grain. They should not be used for cohesive bulk solids. It should also be noted that the draw-down loads on anti-dynamic tubes can be quite high. The computation of these loads and design of location rods has been discussed in Ooms and Roberts (1985) and Roberts (1988b).

Pulsating Loads in Bins – 'Silo Quaking'

As is often the case, the solution of one problem which leads to an improvement in plant performance exposes other problems which require further research and development. In terms of silo loads, a re-occurring problem is the phenomenon of 'silo quaking', a term used to describe pulsating loads which may be experienced during discharge. If the frequency of the flow pulsations is in harmony with any of the natural frequencies of the structure, severe dynamic loads and stresses can occur. The problem of 'silo quaking' is discussed in Roberts et al (1991); Roberts (1993,1994); and Craig and Roberts (1994). The discussion that follows provides an overview of the 'silo quaking' problem as it relates to mass-flow, funnel-flow, expanded-flow and intermediate-flow bins.

The silo quaking problem

Tall mass-flow and funnel-flow bins

The flow characteristics in mass-flow bins are illustrated in Figure 22. As discussed in **Free flowing granular materials**, there is a minimum level H_{cr} which is required to enforce

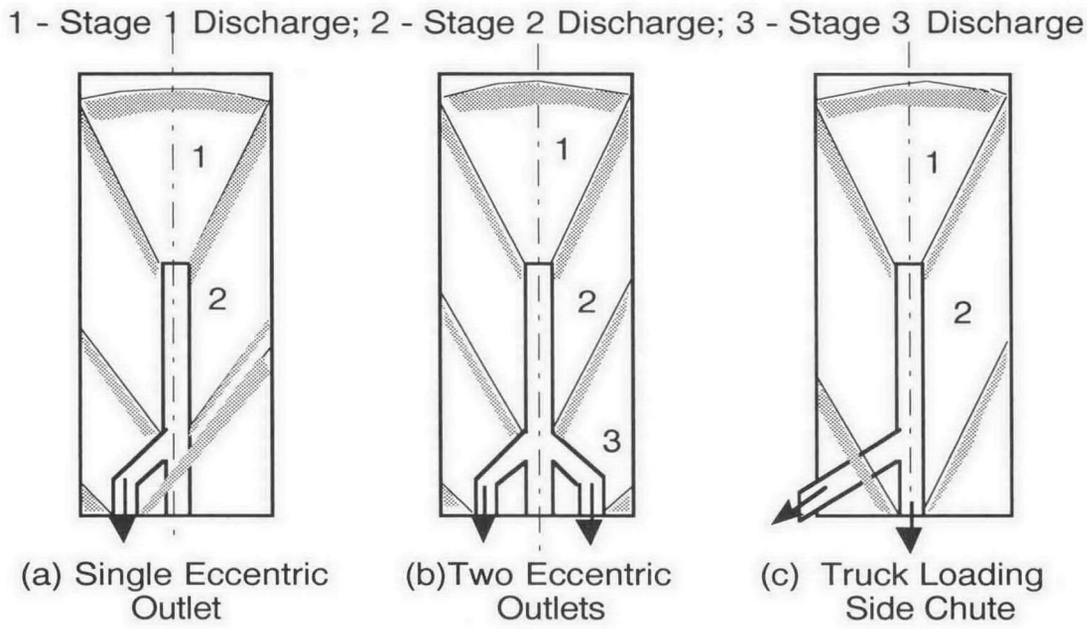

Fig. 21. Applications of the anti-dynamic tube for eccentric discharge.

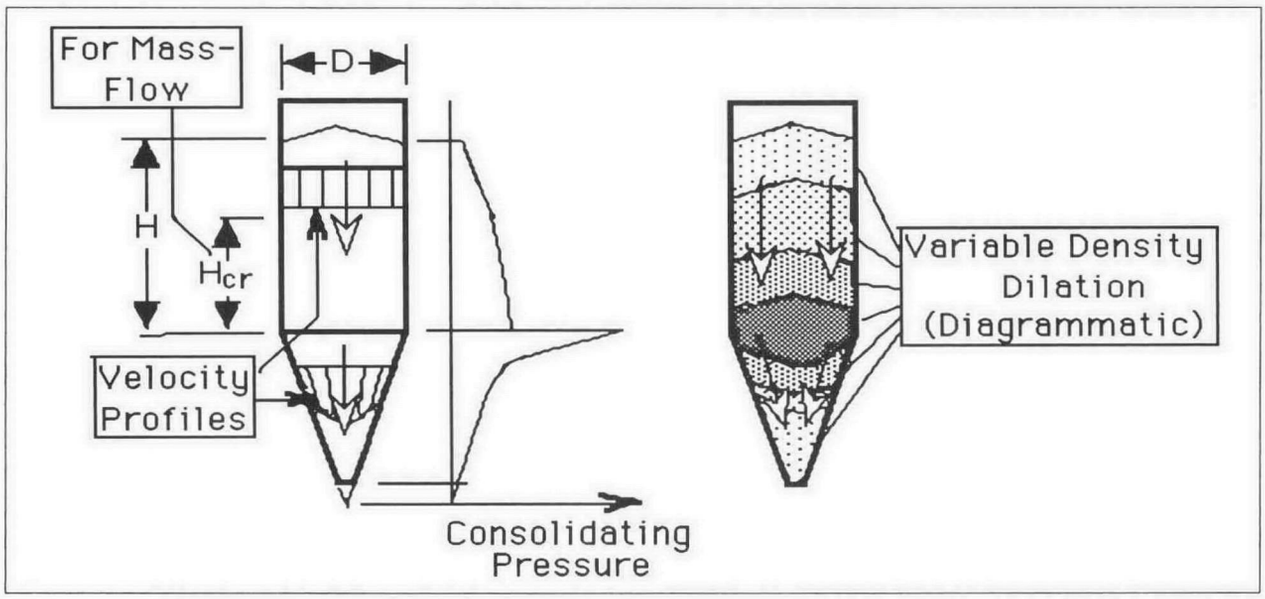

Fig. 22. Mass-flow bin, (a) velocity profiles and pressure distribution; (b) variable density and dilation.

mass-flow in the hopper. Typically, this height ranges from approximately 0.75 D to 1.0 D. As the material flows, it dilates leading to variations in density from the static condition. This is depicted pictorially in Figure 22b. With $H > H_{cr}$, the flow in the cylinder is uniform or 'plug-like' over the cross-section, with flow along the walls. In the region of the transition, the flow starts to converge due to the influence of the hopper and the velocity profile is no longer uniform. The velocity profile is further developed in the hopper as shown. As the flow pressures generate in the hopper, further dilation of the bulk solid occurs. As a result of the dilation, it is possible that the vertical supporting pressures decrease slightly reducing the support given to the plug of bulk solid in the cylinder. This causes the plug to drop momentarily giving rise to a load pulse. The cycle is then repeated.

A similar action to that described above may occur in tall funnel-flow bins or silos where the effective transition intersects the wall in the lower region of the silo. As a result, there is flow along the walls of a substantial mass of bulk solid above the effective transition.

Funnel-flow and expanded-flow bins

During funnel-flow in bins of squat proportions, where there is no flow along the walls, as depicted in Figure 23, dilation of the bulk solid occurs as it expands in the flow channel. As a result some reduction in the radial support given to the stationary material may occur. If the hopper is fairly steeply sloped, say ($\theta \geq \delta$), then the stationary mass may slip momentarily causing the pressure in the flow channel to increase as a result of the 'squeezing' action rather like that of a collet used to clamp a rod of steel in a lathe. The cycle then repeats, the flow being characterised by a 'ratchet' type effect.

Expanded-flow bins are commonly used to store bulk solids in large tonnages. Pulsating loads, illustrated in Figure 24, can occur in such bins, particularly if the slope angle θ of the transition is too steep. Pulsating loads can also be experienced in intermediate-flow bins of the type shown in Figure 6. The central flow channel leads to more rapid flow in this region giving rise to pulsating flow due to the 'slip stick' nature of the friction generated at the boundary of the central and outer flow channels.

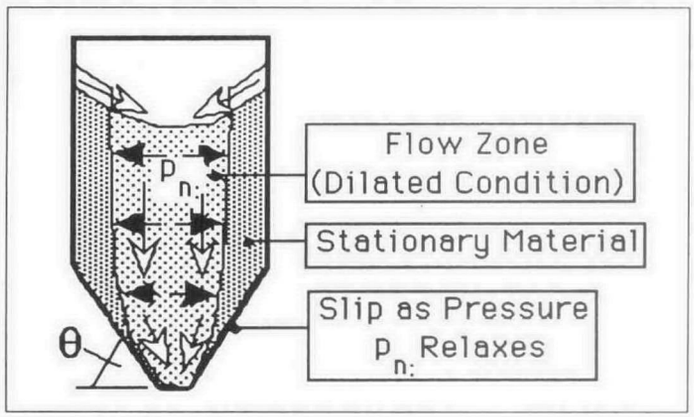

Fig. 23. Funnel-flow bin.

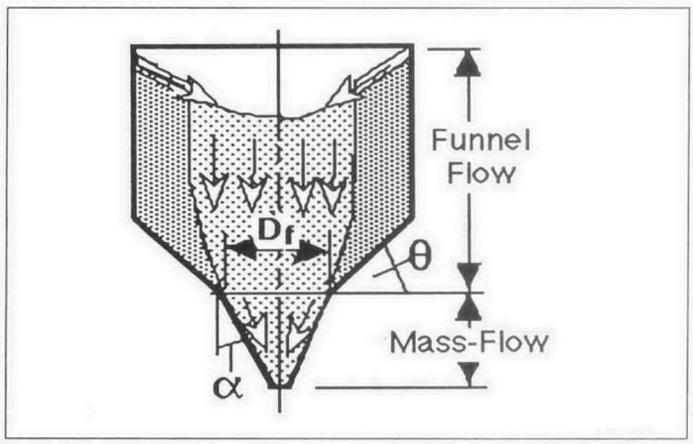

Fig. 24. Expanded-flow bin.

Pilot scale mass-flow bin handling wheat

Studies of pulsating flow have been conducted in the laboratories of The University of Newcastle using a mass-flow test bin (Roberts et al. 1991). The bin is illustrated in Figure 25. It is 1.2 metre diameter with a 3.5 metre tall cylindrical section constructed of mild steel; the conical mass-flow hopper is constructed of stainless steel. The bin is fitted with load cells which measure, simultaneously, both normal pressure and shear stress.

By way of illustration, typical test results using wheat are presented. Fourteen load cells, located as shown in Figure 25, are capable of measuring both normal pressure and wall shear stress. For the purpose of the present discussion on load pulses, the loads acting in the cylinder are examined. A series of tests were conducted for different stored heads in which the normal pressures and shear stresses at several locations were recorded during filling, during undisturbed storage and during emptying. Referring to Figure 25, the locations at which the measurements are reported are 5, 7, 10, 12, 13 and 14. Three head heights of the wheat in the cylinder were examined:

H = 3.44 m	2.41 m	1.1 m
H/D =2.9	2.0	0.9

Pressures pulsations during settling after filling

A dynamic 'slip stick' effect was observed in both the normal pressure and shear records during filling and during settling after filling. By way of example Figure 26, shows sample records for location 14 for the ratio H/D = 2.9. A dynamic 'slip stick' effect is depicted in both the normal pressure and shear records during filling; this effect continues on after the bin is filled, the effect being most pronounced in the shear stress record where the pulses are most evident. It is quite clear that during undisturbed storage, the stored mass approaches, asymptotically, its critical state consolidation condition by a pulse type settling action. The phenomena depicted in Figure 26 was observed at all locations, with the pulses at each location occurring at the same time intervals. Records of the undisturbed settling were taken over prolonged time periods. The same effect was observed for the three H/D ratios examined. As the settling time increased, the pulse period also increased in an exponential manner as illustrated in Figure 27. This shows that the settling characteristics for the two cases H/D = 2.9 and H/D = 2.0 are virtually the same.

Pressures during emptying

Figure 28 shows for H/D = 2.9, the normal wall pressures and shear stresses at locations 5 and 14. At location 5, the dynamic wall pressure and shear stress have each taken approximately one minute to reach their maximum values. At this location, which is near the hopper transition, the long rise time is no doubt associated with the time taken to establish the arched stress field in the hopper. The influence of a pulsating flow effect is depicted in the records for location 5, as for all other locations, even though the amplitude of the pulsations in the normal pressure and shear stress at location 5 is small compared with the average values. The amplitude increased relative to the average values at higher locations in the bin. For instance, as Figure 28b shows, at location 14, the pulsations

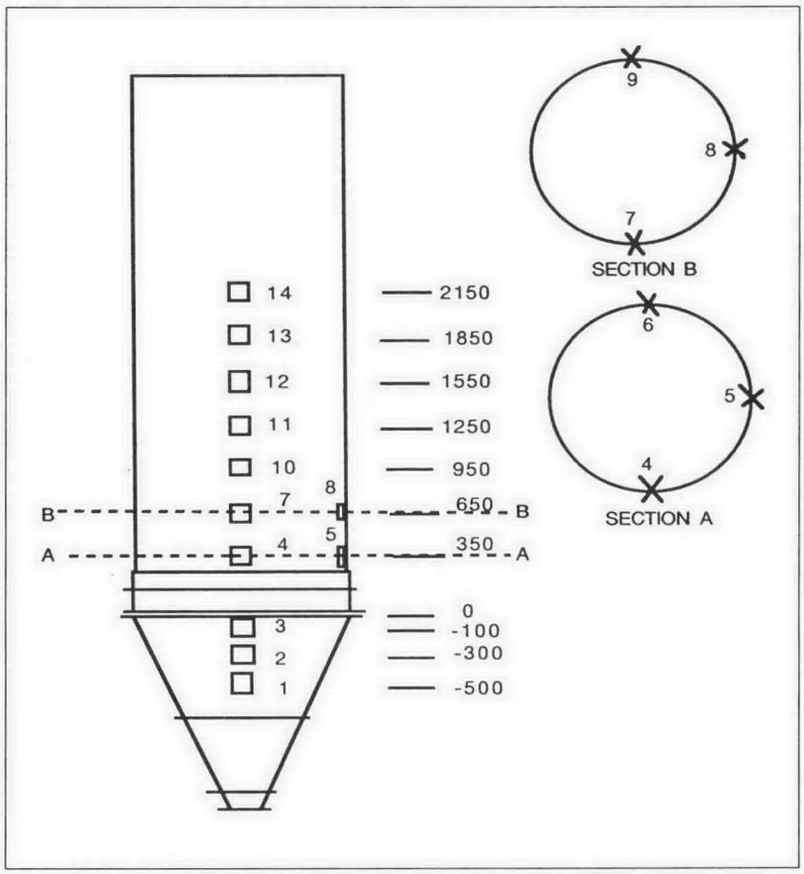

Fig. 25. Mass-flow test bin.

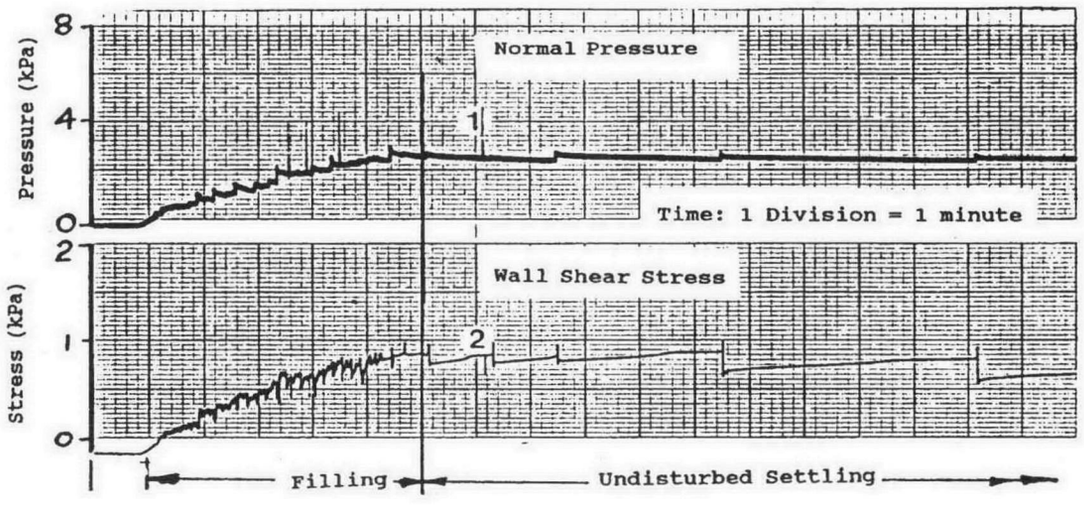

Fig. 26. Normal pressure and shear stress records for wheat at location 14 of test bin

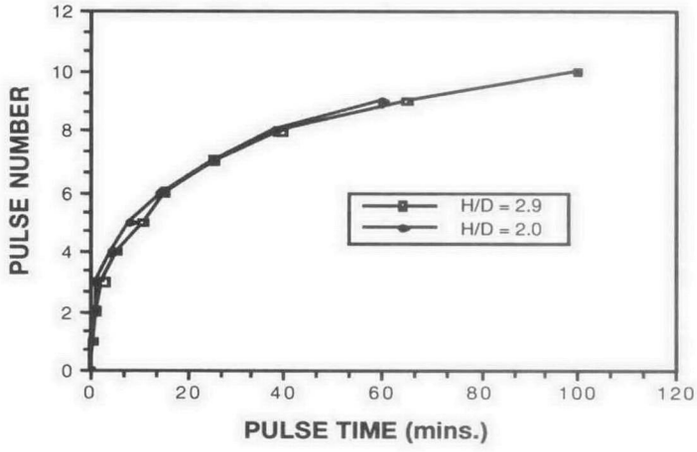

Fig. 27. Load pulsations during undisturbed storage of wheat in test bin.

(a)

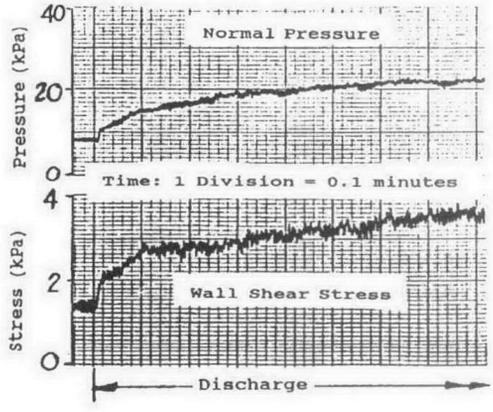

(b)

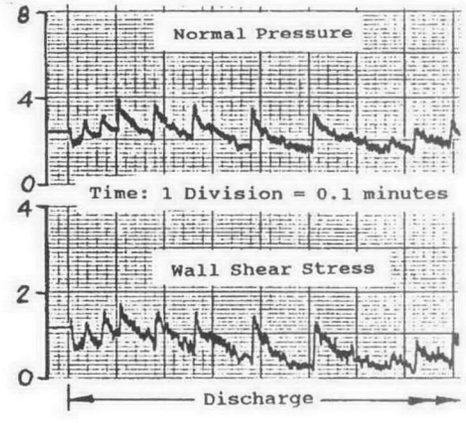

Fig. 28. Pressures and shear stresses for wheat during emptying $H/D = 2.9$. (a) Results for location 5 (b) Results for location 14.

are quite pronounced, the period of the pulsations averaging approximately 5 seconds.

Effect of surcharge head

Similar dynamic effects were experienced for the case of $H/D = 2.0$, but when the head was reduced to $H/D = 0.9$, there was no evidence of any pulsations during discharge. This confirms the conclusion that self excited pulsating flows in mass-flow bins which give rise to the 'silo quaking' phenomenon are associated with surcharge heads greater than a minimum value of, say, $H/D = 1.0$.

$$\text{Perimeter } P = (2)^{1-m}(\pi)^{m}(L)^{1-m}(D)^{m+1} \tag{18}$$

Dynamic loads in tall mass and funnel-flow bins

Roberts(1993) developed a simplified theory to determine the magnitudes of the dynamic loads due to 'silo quaking'. The loading conditions are depicted in Figure 29.

Shock loads

It is postulated that due to 'silo quaking' shock loads are imposed on a plane at some location in the cylinder wall. While there may well be several shock planes, the case of a single shock plane occurring at a height H_{cr} in the cylinder is considered as the worst possibility as far as loading is concerned. Above this plane, the bulk solid is considered to behave as a plug which imparts step loads due to 'slip-stick' motion as may arise from variations in density and in wall friction, as the friction changes from limiting or static to kinetic values. The behaviour is illustrated in Figure 29.

After each shock occurs, the dynamic wave will decay with time according to the bulk elastic properties and damping characteristics of the consolidated bulk solid. It is assumed that the amplitude of the shock pressure Δp_{wy} normal to the wall will decay exponentially with distance measured on each side of the shock plane. That is,

$$\Delta p_{wy} = \Delta p_{wo} e^{-\mu K y/R} \tag{13}$$

Where the maximum increment Δp_{WO} in lateral wall pressure is given by

$$\Delta p_{wo} = \frac{F_D}{A} K \tag{14}$$

Equation (13) may be used to estimate the peak dynamic pressures due to silo quaking. Δp_{wy} is the additional wall pressure applied to the initial or static wall pressure p_{ni} as indicated in Figure 29 (b). As $y \rightarrow h$, it is assumed that Δp_{wy} 'tails off' to approach the flow pressure at the top surface in the cylinder.

F_D is the total shock load and acts over the cross-sectional area A. F_D is given by

$$F_D = k_d \left\{ \frac{W}{h}\left[1 - e^{-\mu K h/R}\right]\left[\frac{R}{\mu K} - h_s\right] + W_s \right\} \tag{15}$$

The two weight components are

$$W = \rho P R h \tag{16}$$

$$\text{and } W_S = \rho P R h_S \tag{17}$$

where

$\gamma = \rho g$ = bulk specific weight, kN
ρ = bulk density, t/m^3
P = perimeter of flow channel, m
R = effective radius, m
h = head, m
h_S = surcharge head,
k_d = Dynamic load factor

$$\text{Effective radius } R = \frac{D}{2(1+m)} \tag{19}$$

$$\text{Surcharge head } h_s = \frac{H_s}{m+2} \tag{20}$$

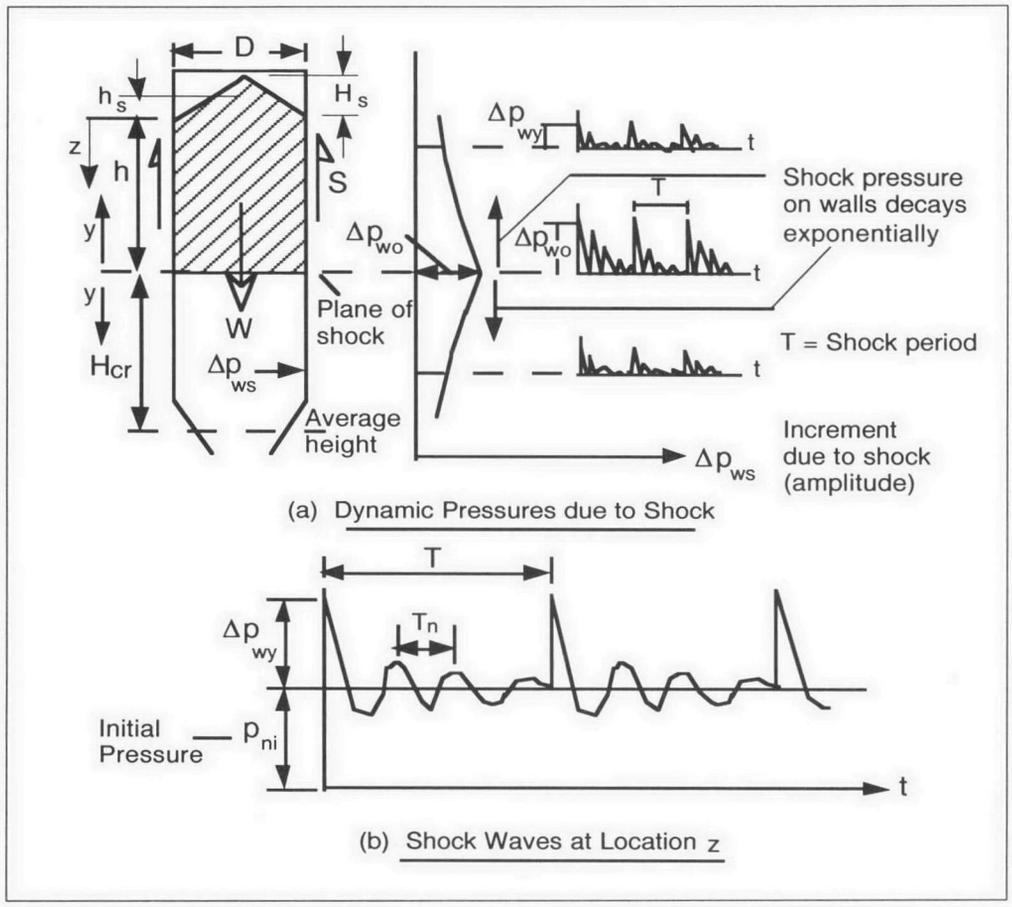

Fig. 29. Dynamic loads induced in silo.

where
$m = 0$ for plane-flow
L = length of flow channel,
$m = 1$ for axi-symmetric flow
D = diameter or width of flow channel
H_S = actual surcharge head
h_S = Effective surcharge head

If the load F_D is suddenly applied at each pulse period, then $k_d = 1.0$. Under severe conditions, such as when the moisture content of the bulk solid is high, the 'slip stick' effect is likely to be more pronounced. In this case $k_d > 1.0$.

Wave motion—brief discussion

The natural frequencies of the stored material are given by

$$f_i = \frac{i\lambda}{4h} i = 1,3,5..... \quad (21)$$

where λ = wave velocity such that

$$\lambda = \sqrt{\frac{E}{\rho}} \quad (22)$$

E = elastic modulus of bulk solid
ρ = bulk density

The wave velocity for the bulk solid will depend on the properties of the bulk solid including the consolidation conditions and moisture content. It has been determined, for example, that for a certain dry bulk solid material, λ ranges from 250 to 400 m/second. Assuming λ = 300m/second, then the natural frequencies will be $f_i = {}^{75}/_{h}\ {}^{225}/_{h}\ {}^{375}/_{h}$...(Hz) for i = 1,3,5.. respectively. For instance if h = 10 m, this gives f_i = 7.5, 22.5, 37.5... Hz. With low damping, the fundamental period T_n = 0.133 seconds; the period will increase as damping increases.

Effect of reducing head due to discharge

It is assumed that the location of the shock plane remains substantially at the critical height H_{cr} during discharge. Therefore, as the level in the bin drops, h decreases and the amplitudes of the shock pressure normal to the wall, Δp_O and Δp_S, also decrease. When the level drops to the critical height H_{cr}, h = 0 and the shock pulses virtually disappear. The number of cycles of dynamic load due to 'silo quaking' during *each* discharge is obtained from the equation

$$\text{Number of pulses per discharge cycle} = \frac{\text{Time to discharge to critical height } H_{cr}}{\text{Pulse period T}}$$

It is also noted from equation (17) that, as h (Figure 8) decreases, the natural frequencies of the stored bulk solid will increase.

Period of pulses

As shown by Roberts (1993), the pulse period may be estimated from the following relationship

$$T = \left(t_o + \tfrac{v}{a}\right) + \sqrt{\tfrac{v}{a}\left(2t_o + \tfrac{v}{a}\right)} \quad (23)$$

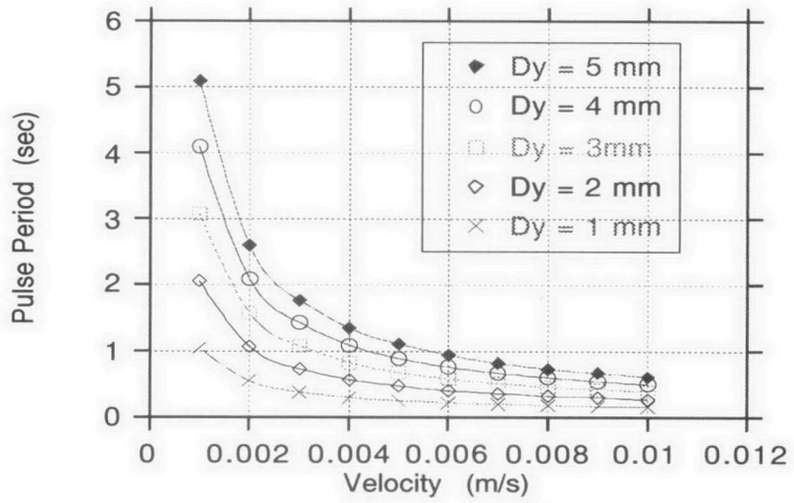

Fig. 30. Pulse period versus velocity a = 1 m/second^2

where

$$a = \frac{F_D g}{W_T} \tag{24}$$

$$v = \frac{Q}{\rho A} \tag{25}$$

$$A = \left(\frac{\pi}{4}\right)^m (L)^{(1-m)} (D)^{(m+1)} \tag{26}$$

$$t_o = \frac{\Delta\varepsilon_y}{v} \tag{27}$$

The variables given by equations (23) to (27) are defined as

a = acceleration of upper mass during pulse motion, m/second^2

v = average velocity of bulk solid in the cylinder during discharge, m/second

Q = discharge rate, kg/s

A = cross-sectional area of cylindrical section of bin

F_D = dynamic force defined by equation (10)

W_T = total weight of upper mass, N

t_o = time for motion of upper mass to be initiated

$\Delta\varepsilon_y$ = expansion of consolidated mass in vertical direction due to dilation

The parameter $\Delta\varepsilon_y$ is difficult to determine precisely. It is dependent on properties of the bulk material including the degree of consolidation and the particle size distribution. The acceleration given by equation (24) will always be less than the gravitational acceleration, since $F_D < W_T$. For the acceleration a = 1 m/second^2, which is a typical value, the variation of the expected pulse period T with the average velocity v for various values of $\Delta\varepsilon_y \equiv Dy$ is shown in Figure 30. This indicates the velocity dependency characteristic of the pulse period. As indicated, the pulse period is relatively insensitive to average velocity for velocities above 0.004

Example—Pilot scale wheat silo of Figure 25

To illustrate the application of the theories presented, reference is made to the experimental silo investigation described in Section 3. The following data apply:

D = 1.2 m

H = 3.44m

$H_s = 0$

$\mu = \tan 30^o = 0.577$

$K = 0.4$

H_{cr} = 1.4 m (assumed)

$h = 1.5$

Q = 5 t/hR =

$F(D/4)$ = 0.3 m

ρ = 0.85 t/m^3

Amplitude of Normal Pressure

Equation (16) : W = 18.9 kN

Equation (15): F_D = 9.6 kN

Equation (14): Δp_{wo} = 3.4 kPa

In order to compare the predicted and measured results for the load cell location 14 of Figure 25, equation (13) is used noting that y = 2.15 - 1.2 ≈ 1.0 m. This gives Δp_{wy} = 2.06. From Figure 28, the measured value of $\Delta p_{yo} \approx$ 1.9 kPa which is in reasonably close agreement with the predicted value.

Pulse period

Assuming that $\Delta\varepsilon$ ranges from 5 to 7 mm for the wheat, using equations (19) to (23), the estimated pulse periods are, respectively, T = 3.5 seconds and T = 4.9 seconds. From Figure 28, the actual pulse period ranges from 2 to 7.5 seconds averaging around 5 seconds. On this basis it is concluded that equation (19) is a reasonable predictor of the pulse period.

Squat funnel, intermediate and expanded flow bins

The effective dynamic mass of bulk solid in the central flow channel of the hopper section is the total mass in this section less the frictional support due to shear at the boundaries between the central and outer flow channels. This is depicted in Figure 31.

Here the analysis is similar to that presented for tall bins, except in this case the flow pulsations are generated in the lower hopper section. The pulsating mass is as indicated in Figure 11. Equations (15) to (20) apply in this case with the following substitutions:

$D_f = D$ = width or diameter of flow channel and

μ = coefficient of internal friction of bulk solid

Normally $\tan \phi_t \geq \mu \geq \sin \delta$ (26)

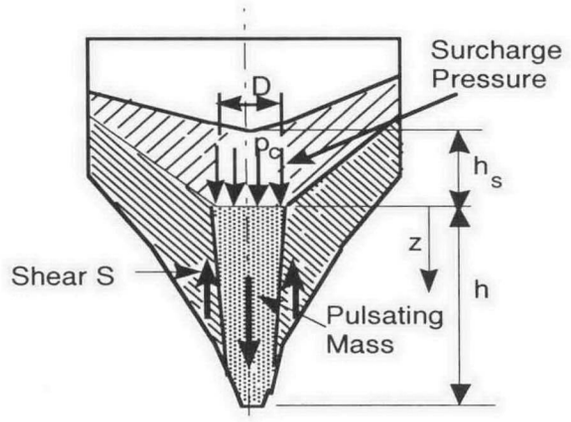

Fig. 31. Effective mass in pulsating flow.

where ϕ_t = static angle of internal friction and δ = effective angle of internal friction

Silo quaking problem—two case study examples

Field observations confirm the foregoing description of the mechanisms of 'silo quaking' (Roberts et al. 1991; Roberts 1993, 1994). For illustration purposes, two case study examples of pulsating flow in bins are presented. While the examples refer to coal bins, the observations could be equally applicable to grain.

Tall silos with chisel-shaped hoppers

Severe silo quaking problems were experienced in an installation of three, 12700 t, reinforced concrete coal silos. The silos, which are shown schematically in Figure 32, stand 58 m above the ground; the height above the base is 52 m, the internal diameter is 21.4 m and the wall thickness is 0.3 m. Adjacent silos are connected by concrete along the vertical lines of intersection. The silos have chisel-shaped, plane-flow hoppers lined with carbon steel plate, the half angle α being 40°, this being the angle with respect to the vertical. The hopper splits into three outlets, the lower hoppers being lined with stainless steel. The maximum discharge rate is 2700 t/hour through vibratory feeders. The reported period of the shocks was 3 –5 seconds, the shock loading being most severe when the silos were substantially full. After several years of use, severe damage started to occur, with sections of concrete being dislodged, particularly at the junction of adjacent silos.

Computation of shock loads

The shock plane is assumed to be located at a height of 26 m above the base of the hopper. The head of coal above the shock plane is $h = 22$ m. Using the procedures presented in Section 4, the following values are calculated:

$W = 77626$ kN

Equation (15): $F_D = 50130$ kN

Equation (14): $\Delta p_{wo} = 56$ kPa

Equation (13) has been used to compute the locus of the shock pressure amplitude, the results being illustrated in Figure 33. Also shown are the static and flow pressures. In view of the curved transition of the chisel-shaped hopper with the cylinder, the pressure profiles will vary around the periphery of the bin. Figure 13 applies to the side of the bin where the chisel-shaped hopper has its highest intersection point with the cylinder wall.

Estimation of pulse period

The application of equations (19) to (23) give the following predicted values of the pulse period:

For discharge rate $Q = 2700$ t/hour; $T = 2.4$ seconds

These values, which are based on $\Delta\varepsilon = 5$mm for the coal, are in general agreement with the approximate values of 3–5 seconds as reported for the actual silo.

Vibration of structure

A critical factor in the operation of the silos is the influence of the dynamic characteristics of the overall structure. Noting that the silos are supported on columns on a base, which, in turn, is supported on piles, a simplified dynamic model of the silos is shown schematically in Figure 34. There will be vertical and lateral stiffness due to the columns and piles as well as vertical and lateral stiffness due to the concrete connecting adjacent silos. In view of the significant variation in the silo mass from the full to the empty condition, there is a significant variation in the natural frequencies.

The natural frequency for the fundamental mode is given by

$$\omega_n = \sqrt{\frac{k}{M}}$$

Noting the variation in mass, the natural frequency of each silo will change as follows:

$$\frac{\omega_n full}{\omega_n empty} = 0.57$$

The natural frequency of the full silo is only 0.57 of the empty silo. While the various stiffness values of the structures are not known, it is possible that the load pulse frequency of 3 to 5 seconds could excite one of the silo modes. As each silo fills and empties, there will be different mass contents and, hence, different frequencies for adjacent silos. As a result, there will be dynamic coupling between adjacent silos which could impose significant loads on the concrete connecting these silos.

The modes of vibration, while complex, would involve a combination of vertical and sideways swaying motion, the latter induced by non-symmetrical loadings of coal in the silos as well as variations in ground stiffness in the zone of the supporting piles.

Multi-outlet bins

Silo-quaking problems have been known to occur in bins with multiple outlets. By way of illustration, consider the large coal bin shown in Figure 35. The bin has seven outlets, six around an outer pitch circle and one located centrally. The hopper geometries provide for reliable flow permitting complete discharge of the bin contents. Coal was discharged by means of seven vibratory feeders onto a centrally located conveyor belt. When the bin was full or near full, severe shock loads were observed at approximately 3 second intervals during discharge. The discharge rate from each feeder was in the order of 300 t/hour. When the level in the bin had dropped to approximately half the height, the shock loads had diminished significantly. With all the outlets operating, the effective transition was well down towards the bottom of the bin walls and the critical head H_m was of the same order as the bin diameter and greater than D_F. Substantial flow occurred along the walls, and since the reclaim hoppers were at a critical slope for mass and funnel-flow as determined by flow property tests, the conditions were right for severe 'silo quaking' to occur.

Confirmation of the mechanism of silo quaking was obtained in field trials conducted on the bin. In one series of tests the three feeders along the centre line parallel with the reclaim conveyor were operated, while the four outer feeders were not operated.

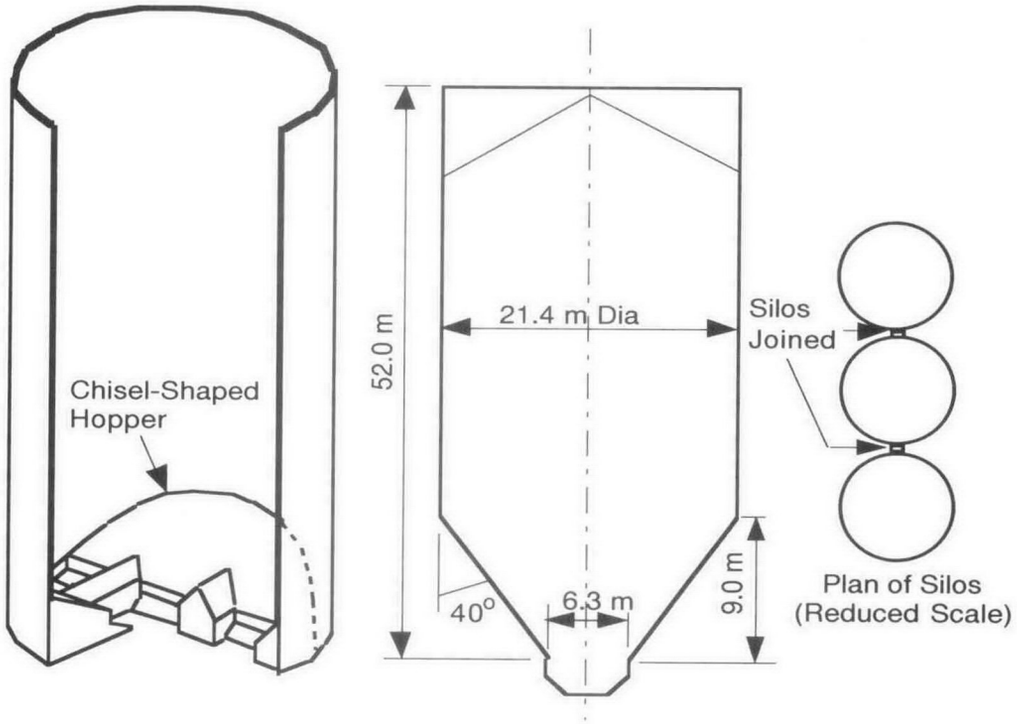

Fig. 32. Tall coal silos

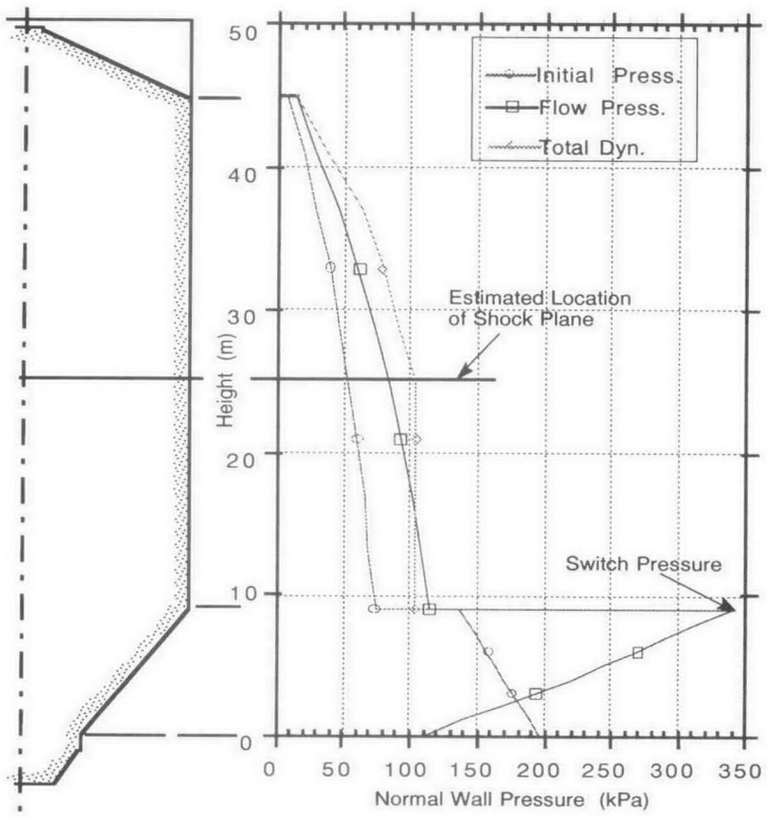

Fig. 33. Pressure distributions for bin.

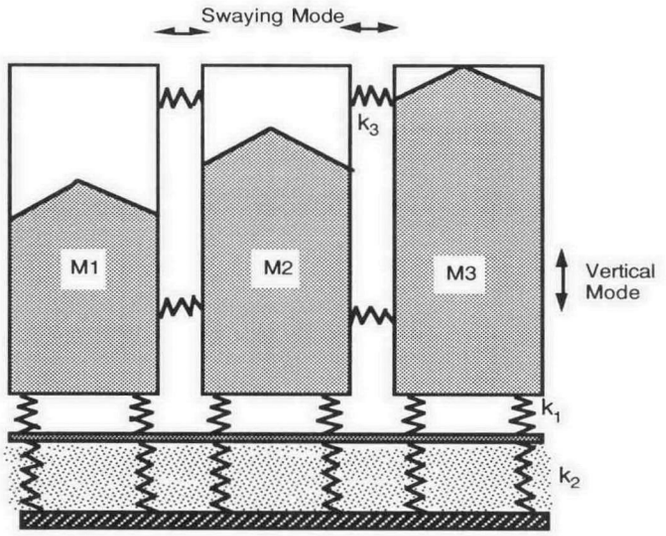

Fig. 34. Simplified dynamic model of silos.

This induced funnel-flow in a wedge-shaped pattern as indicated in Figure 35, with the effective transition occurring well up the bin walls, that is $H_m < H_{cr}$ ($=D_F$) or $H_m << D$. The same was true when only the central feeder (Fdr. 1) was operated; in this case the stationary material in the bin formed a conical shape. Under these conditions, the motion down the walls was greatly restricted and, as a result, the load pulsations were barely perceptible.

In a second set of trials, the three central feeders were left stationary, while the four outer feeders were operated. This gave rise to the triangular prism shaped dead region in the central region, with substantial mass-flow along the walls. The load pulsations were just as severe in this case as was the case with all feeders operating. Dynamic strain measurements were made using strain gauges mounted on selected support columns. When the bin was full (or near full), the measured dynamic strains with $H_m >> H_{cr}$ were in the order of 4 times the strains measured when the flow pattern was controlled so that $H_m < H_{cr}$.

Concluding Remarks

This paper has presented an overview of some recent developments in the technology of bulk solids handling as it relates to the grain industry. The paper has focused on silo design, emphasising the need to understand the relevant properties of the grain and how these relate to silo geometry and discharge flow patterns to generate the load patterns exhibited in the silo walls. While the loading patterns in the case of symmetrical silos are well defined, in the case of multi-outlet silos and silos with eccentric discharge the loadings are much more complex leading to bending and buckling stresses in the walls.

With the emphasis on grain conditioning procedures, such as aeration, to control grain quality, it is important to also take note of the influence of any such grain conditioning on the bulk storage and flow properties of the grain. In this respect, increased moisture content which produces grain swelling can cause substantial increases in silo wall loads. Daily and seasonal fluctuations in temperature which cause expansion and contraction of silo walls, particularly in the case of steel silos, can also cause substantial silo wall pressure fluctuations leading to increased loads during periods of contraction and structural fatigue.

Methods of controlling loads in tall, single and multi-outlet silos have been discussed. Particular mention has been made of the use of anti-dynamic tubes to control the flow pattern and, hence, control the magnitude of the wall pressures generated during discharge.

A re-occurring problem in bins and silos is the phenomenon of 'silo quaking', a term used to describe pulsating loads which may be experienced during discharge. The various mechanisms of 'silo quaking' have been outlined and methodologies to determine the magnitude and distributions of the dynamic loads have been reviewed. If the frequencies of the flow pulsations are in harmony with any of the natural frequencies of the structure, severe dynamic loads and stresses can occur.

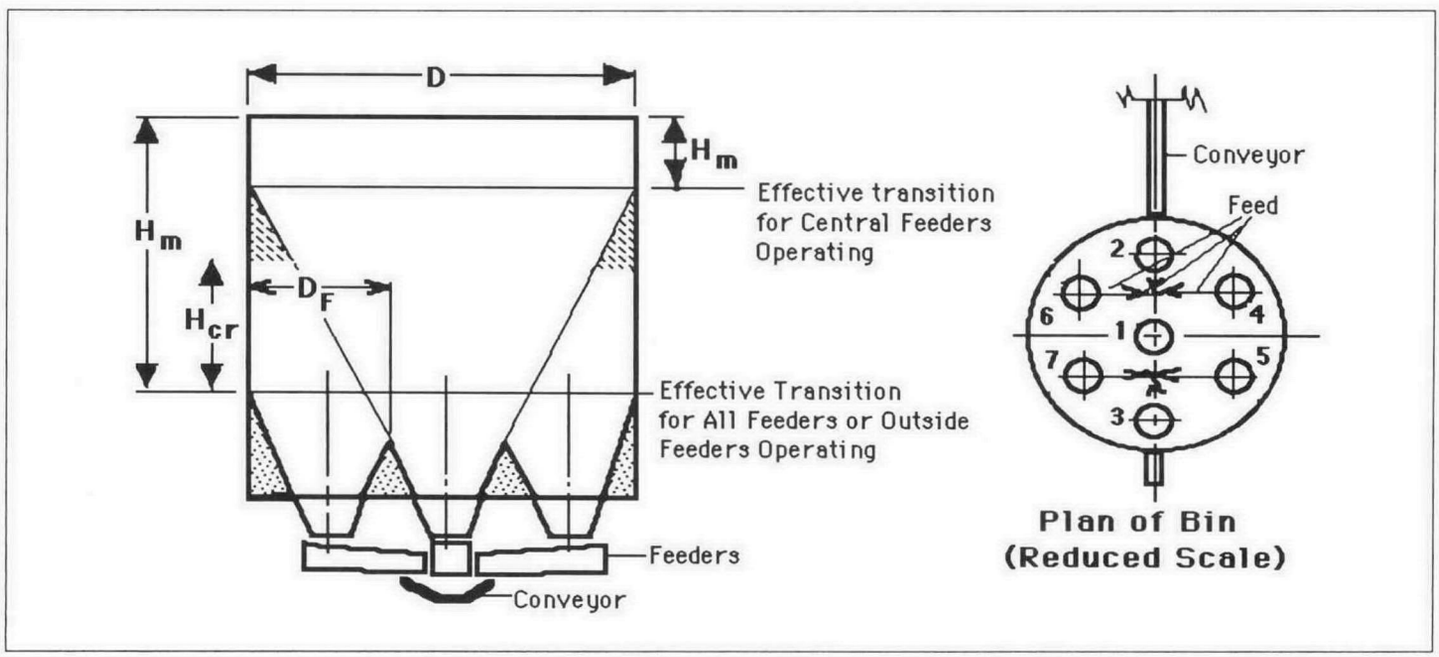

Fig. 35. Multi-outlet coal bin.

It is quite evident that, in recent years, significant advances have been made in research and development associated with bulk handling systems for granular materials. It is gratifying to acknowledge the increasing industrial awareness and acceptance throughout the world and particularly in Australia of modern bulk materials handling testing and plant design procedures. It is also noted that areas for ongoing research are continuing to be identified; provided Universities and research establishments are encouraged to pursue this research, then the future efficiency of bulk materials handling as a key function industry and agriculture is assured.

References

Arnold, P.C. and Roberts, A.W., 1966. Stress distributions in loaded wheat grains, Journal of Agricultural Engineering Research, 11, 1.

Arnold, P.C., McLean, A.G. and Roberts, A.W. 1982. Bulk solids: storage, flow and handling. The University of Newcastle Research Associates (TUNRA), Australia.

Benink, E.J. 1989. Flow and stress analysis of cohesionless bulk materials in silos related to codes. Doctoral Thesis, The University of Twente, Enschede, The Netherlands.

Jenike, A.W. A Theory of flow of particulate solids in converging and diverging channels based on a conical yield function. Powder Tech., 50, 229–236.

Jenike, A.W. 1961. Gravity flow of bulk solids. The Univ. of Utah, Engineering Experiment Station, Bulletin 108, USA

Jenike, A.W. 1964 Storage and Flow of Solids. The Univ. of Utah, Engineering Experiment Station, Bulletin 123, USA.

Jenkyn, R.T., 1978. Calculation of material pressures for the design of silos. Proceedings Institution. Civil Engineers, 2, 65.

Ooi, J.Y. and Rotter, J.M. 1989. Elastic and plastic predictions of storage pressures in conical hoppers. In: Third International Conference on Bulk Materials Storage, Handling and Transportation. Newcastle, Australia, The Institution of Engineers, 203–207.

Ooms, M. and Roberts, A.W. 1985. The reduction and control of flow pressures in cracked grain silos. Bulk Solids Handling, (5), 5, 1009–1016.

Roberts, A.W. 1988a. Modern concepts in the design and engineering of bulk solids handling systems. The University of Newcastle, Australia, TUNRA Bulk Solids Research.

Roberts, A.W. 1988b. Some aspects of grain silo wall pressure research—influence of moisture content on loads generated and control of pressures in tall multi–outlet silos. In: Proceedings Conference, Chicago, USA, May 11–24.

Roberts, A.W. 1993. Mechanics of self excited dynamic loads in bins and silos. Oslo, Norway. Proceedings of the 2nd Reliable Flow on Particulate Solids Symposium 983–1004.

Roberts, A.W and Ooms, M. 1983. Wall loads in large steel and concrete bins and silos due to eccentric and other factors. In: Proceedings 2nd International Conference on the Design of Silo for Strength and Flow, Powder Advisory Centre, U.K. 151–170.

Roberts, A.W., Scott, O.J. and Wiche, S.J. 1991. Silo quaking. A pulsating load problem during discharge in bins and silos. Proceedings Bulk 2000, The Institution of Mechanical Engineers, U.K., 7.12.

Rombach, G. and Eibl, J. 1989. Numerical simulation of filling and discharging processes in silos. In: Third International Conference on Bulk Materials Storage, Handling and Transportation. The Institution of Engineers, Newcastle, Australia, 48–52.

Standards Association of Australia (SAA) 1990. Australian Standard AS3774–1990, Load on bulk solids containers

Thomson F.M. 1984. Storage of particulate solids. Van Nostrand, Handbook on Powder Science and Technology, 9.

Wu, Y.H. 1990. Static and dynamic analysis of the flow of bulk materials through silo. PhD. Thesis, The University of Wollongong, Australia.